

**UNCLASSIFIED**

**AD \_ 405 821 \_**

**DEFENSE DOCUMENTATION CENTER**

**FOR**

**SCIENTIFIC AND TECHNICAL INFORMATION**

**CAMERON STATION, ALEXANDRIA, VIRGINIA**



**UNCLASSIFIED**

NOTICE: When government or other drawings, specifications or other data are used for any purpose other than in connection with a definitely related government procurement operation, the U. S. Government thereby incurs no responsibility, nor any obligation whatsoever; and the fact that the Government may have formulated, furnished, or in any way supplied the said drawings, specifications, or other data is not to be regarded by implication or otherwise as in any manner licensing the holder or any other person or corporation, or conveying any rights or permission to manufacture, use or sell any patented invention that may in any way be related thereto.

405821

6335

ASD-TDR-63-309  
PART I

PEST REACTIONS IN INTERMETALLIC COMPOUNDS  
I. Grain Boundary Hardening in NiGa

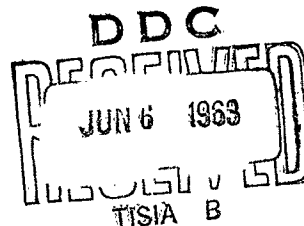
TECHNICAL DOCUMENTARY REPORT NO. ASD-TDR-63-309, PART I  
April 1963

Directorate of Materials and Processes  
Aeronautical Systems Division  
Air Force Systems Command  
Wright-Patterson Air Force Base, Ohio

405821

Project No. 7350, Task No. 735001

(Prepared under Contract No. AF 33(657)-7980  
by the General Electric Research Laboratory, Schenectady, New York;  
A. U. Seybolt and J. H. Westbrook, authors.)



## NOTICES

When Government drawings, specifications, or other data are used for any purpose other than in connection with a definitely related Government procurement operation, the United States Government thereby incurs no responsibility nor any obligation whatsoever; and the fact that the Government may have formulated, furnished, or in any way supplied the said drawings, specifications, or other data, is not to be regarded by implication or otherwise as in any manner licensing the holder or any other person or corporation, or conveying any rights or permission to manufacture, use, or sell any patented invention that may in any way be related thereto.

Qualified requesters may obtain copies of this report from the Armed Services Technical Information Agency, (ASTIA), Arlington Hall Station, Arlington 12, Virginia.

This report has been released to the Office of Technical Services, U. S. Department of Commerce, Washington 25, D. C., for sale to the general public.

Copies of this report should not be returned to the Aeronautical Systems Division unless return is required by security considerations, contractual obligations, or notice on a specific document.

## FOREWORD

This report was prepared by the Metallurgy and Ceramics Research Department, General Electric Research Laboratory, Schenectady, New York, under USAF Contract No. AF 33(657)-7980. The work was initiated under Project No. 7350, "Refractory Inorganic Nonmetallic Materials," Task No. 735001, "Refractory Inorganic Nonmetallic Materials: Non-Graphitic." The work was administered under the direction of the Directorate of Materials and Processes, Deputy for Technology, Aeronautical Systems Division; L. A. Jacobson, 2nd Lt. USAF, was the project engineer.

This report covers work from February 1962 to February 1963.

The authors wish to acknowledge very helpful discussions with many colleagues during the course of the work. In particular, the ideas of John C. Fisher relating to treatment of the diffusion data were very valuable. John W. Cahn assisted considerably in discussions relating to a possible hardening mechanism. We are indebted to Carl Wagner for his suggestion for the measurement of the gallium activity in NiGa.

The thousands of microhardness measurements which comprise such a large part of this study were made by A. J. Peat. Assistance with other phases of the experimental program was provided by J. Godfrey.

## ABSTRACT

The phenomenon of grain boundary hardening recently described by Westbrook and Wood [J. Inst. Metals, 91, 174 (1962-3)] has been explored in detail for the CsCl structure intermetallic compound NiGa. Like many intermetallic compounds, NiGa has a homogeneity range of a few per cent, and it was possible to examine the effect of stoichiometry upon the grain boundary hardening due to preferential oxygen diffusion down grain boundaries. While some grain boundary hardening was noticeable just below 50 A/o Ga, the effect was much less pronounced than at 52 A/o Ga.

By means of microhardness measurements taken along grain boundaries and also transversely to grain boundaries, it was possible to estimate both bulk diffusion and grain boundary diffusion rates for oxygen. In the temperature range 600° to 1000°C, Doxygen seemed to be an insensitive function of temperature for both bulk and grain boundary diffusion.

$$D_{\text{bulk}} = \sim 10^{-12} \text{ cm}^2/\text{sec} \text{ and } D_{\text{g.b.}} = \sim 10^{-5} \text{ cm}^2/\text{sec}$$

While it is not possible to be certain about the hardening mechanism, it seems likely that it is due to a Ga-O complex formed by the reaction  $x\text{O}_{\text{in}} \text{NiGa} + \text{G}_{\text{in}} \text{NiGa} = \text{GaO}_x$ . Such a complex could presumably account for the hardening because of the lattice distortions created.

This technical documentary report has been reviewed and is approved.



W. G. Ramke  
Chief, Ceramics and Graphites Branch  
Metals and Ceramics Laboratory  
Directorate of Materials and Processes

## TABLE OF CONTENTS

	<u>Page</u>
INTRODUCTION . . . . .	1
EXPERIMENTAL TECHNIQUES . . . . .	2
Materials . . . . .	2
Electropolishing . . . . .	3
Hardness Tests . . . . .	4
RESULTS . . . . .	4
Incidence of Hardening in NiGa . . . . .	4
Effects of Atmosphere . . . . .	5
Effects of Composition . . . . .	5
Effects of Heat Treatment . . . . .	7
KINETICS OF THE HARDENING REACTION IN NiGa, 52 A/o Ga . . . . .	10
OXYGEN PENETRATION STUDIES . . . . .	13
CALCULATION OF OXYGEN DIFFUSION CONSTANTS . . . . .	17
STABILITY OF THE HARDENING REACTION . . . . .	20
METALLOGRAPHY . . . . .	23
DEFECT STRUCTURE OF NiGa . . . . .	23
THERMODYNAMICS OF THE GALLIUM OXIDES . . . . .	25
ACTIVITY OF GALLIUM IN NiGa . . . . .	26
EFFECT OF OXYGEN ON NiGa STRUCTURE . . . . .	32
GENERAL DISCUSSION . . . . .	34
CONCLUSIONS . . . . .	36
REFERENCES . . . . .	37

## LIST OF ILLUSTRATIONS

Figure	Page
1. Hardness of grains (g) and grain boundaries (g.b.) after 2 hours at 900°C, O <sub>2</sub> , quenched, plus indicated times at 700°C for 48.6, 49.6, 51.6 A/o Ga. . . . .	6
2. Hardness of grain and grain boundaries as a function of soaking time at 900°C in air, followed by air cool (52 A/o Ga). . . . .	7
3. Hardness of grain boundaries after 2 hours 900°C, O <sub>2</sub> , quenched, then aged at indicated temperatures for periods of time in minutes noted at each point (52 A/o Ga). . . . .	9
4. Rate of hardening at 700°C (52 A/o Ga). . . . .	11
5. VHN vs square root of time (52 A/o Ga). . . . .	11
6. Time in minutes required to reach 450 VHN as function of temperature (52 A/o Ga). . . . .	12
7. Grain boundary and bulk hardness as a function of distance from the gas-metal interface. 52 A/o Ga alloy heated at 1000°C for 16 1/2 hours in oxygen. . . . .	14
8. VHN vs distance from grain boundary at two depths from the gas-metal interface. 52 A/o Ga alloy heated for 4 hours at 900°C in oxygen. . . . .	15
9. Hardness contours originating from surface oxide films formed at 700°C, followed by 4 hours 900°C vacuum treatment (52 A/o Ga alloy). . . . .	16
10. ΔH along a grain boundary vs distance from surface. . . . .	19
11. Effect of heat treatments on the hardness contour of a sample heated to 900°C, O <sub>2</sub> for 2 hours. . . . .	21
12. 52 A/o Ga in hardened state, etched HCl + CrO <sub>3</sub> . 1000X . . . . .	23
13. Density and lattice parameter of NiGa vs composition. . . . .	24
14. Free energy of formation of Ga <sub>2</sub> O and Ga <sub>2</sub> O <sub>3</sub> per gram atom of oxygen as a function of temperature. . . . .	26
15. Solid electrolyte galvanic cell. . . . .	28
16. Activity of gallium in NiGa as a function of composition. . . . .	31
17. Partial molal free energy of gallium in NiGa at 835°C as a function of composition. . . . .	32

## PEST REACTIONS IN INTERMETALLIC COMPOUNDS

### I. Grain Boundary Hardening

A. U. Seybolt and J. H. Westbrook

#### INTRODUCTION

The susceptibility of certain intermetallic compounds to serious intergranular attack when heated in the air at certain temperature levels (often referred to as the  $\text{MoSi}_2$  "pest") is rather well established. Perhaps the best-known example is  $\text{MoSi}_2$ , a compound which has been used considerably in recent years both as a coating material for molybdenum and as a solid heating element for high-temperature furnaces ("Super-Kanthal"). At high temperatures, this silicon-rich compound oxidizes to an amorphous  $\text{SiO}_2$  at the surface, producing a very stable coating which does not grow much in thickness even after many hours of high-temperature operation. However,  $\text{MoSi}_2$  and other analogous compounds such as  $\text{WSi}_2$  have been found to become seriously embrittled when held at temperatures around  $550^\circ$  to  $800^\circ\text{C}$  in the air. The cause of the embrittlement has not been clearly established.

Recently Westbrook and Wood<sup>(1)</sup> observed that grain boundary segregation of oxygen and/or nitrogen (as well as other impurities) in intermetallic compounds resulted in intergranular embrittlement which could be detected by a difference in the microhardness of grain boundary regions relative to the interior of the grains. They found that such local hardening was common to a wide variety of intermetallic compounds where one component was appreciably more electropositive than the other. They also reported that grain boundary hardening was only observable with a stoichiometric excess of the electropositive component, even in a phase-pure sample, and that the degree of hardening was affected also by heat treatment. These observations were supported by detailed studies<sup>(2)</sup> of the CsCl structure compounds  $\text{AgMg}$  and  $\text{NiAl}$ . Later,<sup>(3)</sup> they suggested a mechanism by which such segregation could account for the "pest" type of degradation. Briefly, the "pest" temperature range is held to be that which permits preferential grain boundary diffusion of oxygen and/or nitrogen from the ambient atmosphere and simultaneous segregation of the gaseous element at or near the grain boundaries. Structural disintegration then occurs by the action of internal stresses on these embrittled regions. A close correlation was observed in each case between the temperature at which grain boundary hardening disappeared and the upper temperature limit of the "pest" effect in the compounds  $\text{NiAl}$ ,  $\text{MoSi}_2$ , and  $\text{ZrBe}_{13}$ .

In addition to the necessity of oxygen or nitrogen contamination and the effects of stoichiometry and heat treatment noted above, other general observations were:

1. The grain boundary hardening effect is not confined to a particular compound class (silicides, beryllides, magnesides, etc.,) or crystal structure type although the degree to which structural integrity is lost varies considerably.

2. No second phase is visible at the grain boundary in the usual case even under examination of the boundary surface itself with the aid of the electron microscope.

Grain boundary hardening thus appears to be a necessary condition for a compound to exhibit the "pest" effect although it may not be a sufficient condition. It is also true that saturation of the boundary hardening effect can obtain before significant "pest" degradation has taken place. In any event, the grain boundary hardening reaction which was investigated in detail in the compound NiGa during the present study is evidently very similar to the embrittlement observed by Westbrook and Wood in numerous other compounds.

Because of general interest in the phenomenology and effects of impurity segregation, and because of the technological importance of the "pest" degradation, it seems desirable to learn in some detail about the possible operative mechanisms and their kinetics. Microhardness measurement was selected as the principal experimental technique for monitoring segregation. The CsCl structure compound NiGa was chosen for detailed study for a number of reasons:

1. A simple crystal structure,
2. A broad homogeneity range,
3. A modest melting point ( $\sim 1100^{\circ}\text{C}$ ),
4. Oxides of the electropositive element ( $\text{Ga}_2\text{O}$  and  $\text{Ga}_2\text{O}_3$ ) are readily reducible by hydrogen.

The last characteristic was sought since it was anticipated that it would then be possible to reverse the grain boundary hardening by heat treatment, which is not true for compounds containing Mg or Si, for example. Preliminary experiments disclosed that NiGa with excess Ga did exhibit grain boundary hardening, and that the effect could be erased by heating in hydrogen. According to Hansen<sup>(4)</sup> NiGa has a homogeneity range at  $600^{\circ}\text{C}$  and lower from about 48 to 53 A/o Ga. At higher temperatures the homogeneity range is greater. The solidus and liquidus for the 50 A/o alloy are about  $1050^{\circ}$  and  $1170^{\circ}\text{C}$ , respectively.

## EXPERIMENTAL TECHNIQUES

### Materials

Initially, three 50-gram argon atmosphere arc melts were made using carbonyl nickel and 99.99 per cent Ga; the compositions were intended to be 49, 50, and 52 A/o Ga; actual analyses were 48.6, 49.6, and 51.6. Homogenization heat treatments for 48 hours at  $800^{\circ}\text{C}$  in a protective atmosphere were carried out prior to analyses. Oxygen analyses in these alloys varied from 2 to 7 ppm and nitrogen contents were 5 to 9 ppm. No evidence thus far has suggested that the initial spreading gas analyses (as shown above) played a significant role in the results obtained.

The microstructure of the above alloys has shown a single-phase structure with only a very small amount of "dirt" or finely divided second phase. The last has been present in such small amounts as to not warrant any attempt toward identification. The grain size of the as-cast ingots was rather large. An average grain diameter was approximately 1 mm. For some work, some very coarse crystalline material was prepared by the Bridgman technique where the grain size was approximately 5 mm in diameter.

Subsequent to the three small heats referred to above, two additional heats were made which analyzed 52 A/o Ga (180-gram heat) and 51.6 A/o Ga (400-gram heat). These alloys were made by induction melting (argon atmosphere) in a MgO crucible, and were cast into bars about 1/4 by 1 inch in cross section, and a few inches in length. Samples for hardness tests were prepared by cutting off slices with a thin abrasive wheel. In spite of the reported difference in gallium content between these two heats, there appeared to be no difference observable in grain boundary hardening. Most of the later work was done on the alloy last mentioned, while the earlier work was done principally on the 52 A/o material. Because of the very limited amount of the three initial alloys, these were used for only a few experiments.

As the work progressed, other alloys were prepared from the same starting materials, using the same melting practice. The composition of these will be referred to in the appropriate place in the text.

#### Electropolishing

Microhardness measurements on heat-treated samples require removal of any superficial oxide followed by preparation of a metallographic surface. NiGa, like many other intermetallic compounds, shows a great tendency for surface flow and work hardening during mechanical polishing although polycrystalline specimens appear very brittle. Consequently, some preliminary experimentation was required to develop a technique that would yield a clean, flow-free surface with reproducible properties. A standard electropolish was evolved which removed about 27 microns from the surface of the samples and simultaneously lightly etched the sample to reveal grain boundaries. With this procedure, the normal "base" hardness for the interior of grains in the 52 A/o alloy could usually be repeatedly reproduced at about 290 to 300 VHN. Other sources of minor variation in hardness can be attributed to grain size variation and quenching strain. It must be emphasized that with this technique both the grain boundary and bulk hardness values generally reported are for a position slightly below the true gas-metal interface. Even if there were no measurable work hardening effect, some of the surface would have had to be removed to eliminate the surface oxide film.

For the polishing bath a stock solution was prepared as follows: 15 ml HCl, 10 ml HNO<sub>3</sub>, 10 ml CH<sub>3</sub>COOH, plus a pinch of FeCl<sub>3</sub>. In use, this was diluted with about an equal volume of water, the degree of dilution adjusted somewhat to give a suitable polishing rate, depending upon specimen size. The specimen was the anode, connected by a stainless steel probe, and the cathode was a silver strip. Prior to electrolysis the specimens were ground on 400 SiC paper. The voltage was 10, and the current 2.5 to 3 amperes for specimens of about 1/4-inch-square size. The time was about 15 to 30 seconds.

### Hardness Tests

The hardness tests were made using a Kentron microhardness tester, ordinarily with a 25-gram load. The usual procedure was to measure about six points chosen at random at various grain boundaries. Because the surface hardness of the grain interior was always so constant, at least in any one sample, usually only one or two grain-interior readings were taken. Readings at the boundary, taken at different points, rarely disagreed by more than about five points, Vickers hardness number (VHN), although the dispersion was sometimes as much as 10 VHN out of a reading in the range 300 to 500.

When closely spaced hardness readings were desired, as in obtaining a profile of hardness across a grain boundary, 10-gram loads were used. Such light loads were not generally employed because the scatter in hardness readings was appreciably higher in this case. While grain traverses across a grain boundary supply information not obtained by a reading at or close to the boundary, it is also true that traverses (which may require 30 to 40 readings) are very time-consuming, and are not necessary for much of the information required.

The size of the samples used for the various heat treatments was generally quite small, partly because gallium is expensive, and partly because after a few water-quenching treatments the samples broke into several pieces from quenching strains. The samples as cut from the cast bar were usually around 0.080 inch thick by 1/4 by 1/4. Many experiments were successfully made with thinner material, but because of excessive breakage and fragility, it was considered not worth while to attempt to use samples appreciably thinner than 0.060 inch thick for hardness tests.

## RESULTS

### Incidence of Hardening in NiGa

In accordance with the findings of Westbrook and Wood, grain boundary hardening is observed when a sample containing an excess of the electropositive element is:

1. Exposed to a contaminating atmosphere at a high temperature, and
2. Slowly cooled to a low temperature, or
3. Quenched to room temperature and reheated to some intermediate ("aging") temperature.

Preliminary experiments on gallium-rich NiGa disclosed that a few hours exposure at 900°C to an oxygen containing atmosphere provided the requisite contamination and, following quenching from this temperature, minutes of aging at temperatures of the order of 700°C fully developed the grain boundary hardening.

### Effects of Atmosphere

Hardening was observed when the initial heat treatment was conducted in oxygen, air, or in any atmosphere which allowed the formation of a surface oxide film. X-ray examination on many samples showed that the surface film was  $\beta$   $\text{Ga}_2\text{O}_3$ . This film remained quite thin at temperatures near 900°C, and showed characteristic interference colors which varied with film thickness. When the samples were heated in the same temperature range in wet hydrogen or in nitrogen containing traces of moisture or very low partial pressures of oxygen, a comparatively thick, chalky white film was formed, also  $\beta\text{Ga}_2\text{O}_3$ . The reason for the different oxide morphology has not been explored. The question of the presence of  $\text{Ga}_2\text{O}$  and its relative stability with respect to  $\text{Ga}_2\text{O}_3$  will be treated briefly in a subsequent section.

The hardening effect on the grain boundaries was much more pronounced than on the grain centers (or bulk material). However, it will be shown later that quite appreciable surface hardening of the bulk material can occur, particularly with prolonged oxygen heat treatment at temperatures near 900°C. Also, lower temperatures will allow embrittlement of both grain boundaries and bulk, but the time required is longer. The bulk hardening effect is in general restricted to a few microns of the surface (gas-metal interface), but the grain boundary effect is noticeable to depths of 600 microns or somewhat more.

Attempts were made to determine the amount of oxygen absorbed by the samples during the high temperature oxygen heat treatments. However, these efforts were not successful because the amount picked up was so small. Even after many hours exposure to oxygen at 1000°C, vacuum fusion analyses showed only a content of about  $10 \pm 10$  ppm oxygen. Although air and oxygen treatments gave equivalent results, nitrogen played no role in the hardening process as proved by pure nitrogen and ammonia heat treatments. Also, it was noted that heating in a  $\text{H}_2\text{-H}_2\text{S}$  atmosphere corresponding to equilibrium with  $\text{FeS}$  at 900°C showed no hardening effect.

### Effects of Composition

Although some early tests showed the 48.6 A/o Ga and 49.6 A/o Ga heats to be relatively free from grain boundary hardening, a more careful subsequent investigation of these two alloys revealed that the 49.6 A/o Ga alloy did show some hardening, but only with aging times very much longer than those for Ga-rich samples. While stoichiometry is very critical, and the hardening tendency changes rapidly near 50 A/o, a composition can show some hardening when only slightly below 50 A/o in electropositive element.

The increase in hardness of three different alloys is shown in Fig. 1 where both the grain boundary (g.b.) and bulk (g) hardness data are plotted after heat-treating for 2 hours at 900°C in oxygen, quenching, and retreating

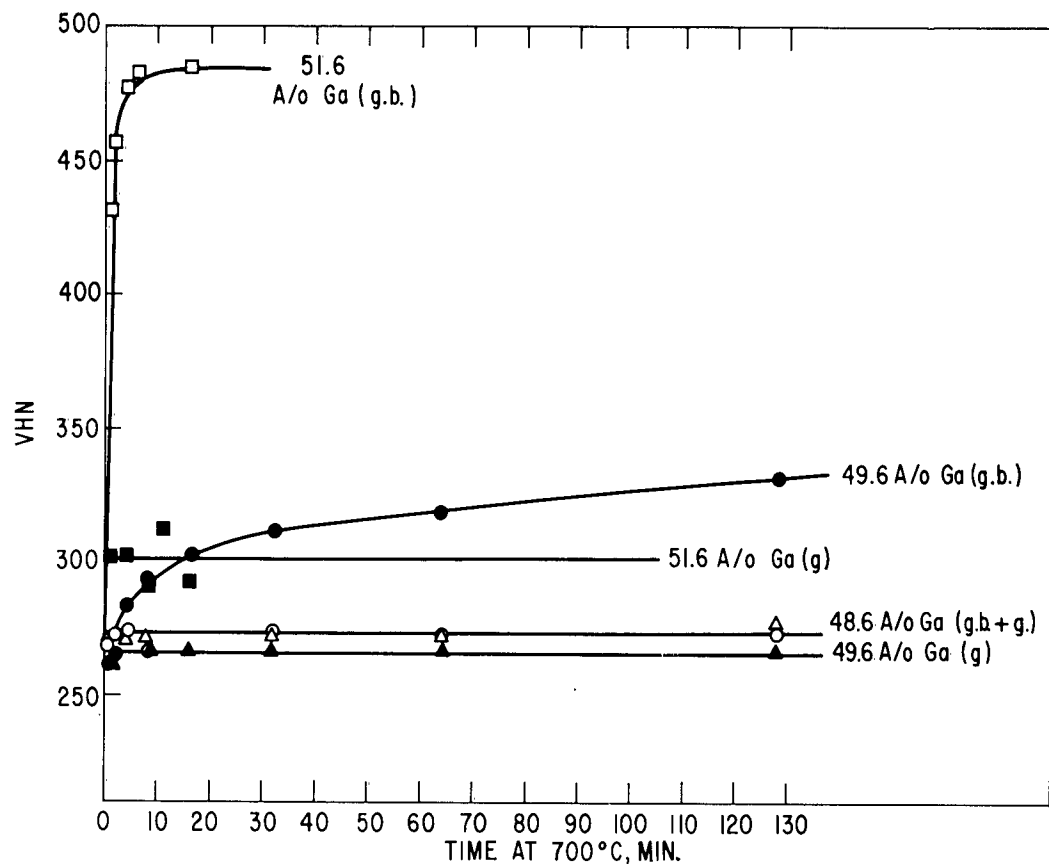


Fig. 1 Hardness of grains (g) and grain boundaries (g. b.) after 2 hours at 900°C, O<sub>2</sub>, quenched, plus indicated times at 700°C for 48.6, 49.6, 51.6 A/o Ga.

for various periods at 700°C. The contrast in behavior between the 51.6 alloy and the others is immediately obvious. As was mentioned above, the bulk of the experiments yet to be described were performed on the 51.6 and 52.0 A/o Ga heats which gave equivalent results.

Although it seems clear that we are concerned with certain effects of oxygen at or near grain boundaries in Ga-rich NiGa, it is not certain whether or not boundaries otherwise differ in composition from bulk material. A few explanatory electron probe tests have been made in an attempt to show some difference in gallium content between grain boundary and grain. Thus far, such tests have been negative. It seems very likely that if there is a higher (or lower) concentration of gallium at the grain boundaries, the effect is too small to be measured readily. The electron probe investigator said that if a difference of 0.1 wt per cent gallium between the bulk and the boundary had been present, it would have been detected.

### Effects of Heat Treatment

It was observed quite early in these studies that the grain boundary hardening was completely eliminated if the NiGa sample were drastically quenched from 900°C or higher. It must be emphasized that the quench must be very fast, as in dropping a small sample of 0.06-inch thickness (or about 0.5-gram weight) into cold water. Quenching into hot water resulted in essentially maximum hardness. The bulk hardness was usually around 300 Vickers Hardness Number (VHN) at the surface, but grain boundary hardness levels could reach about 485. The maximum grain boundary hardness was observed on slow cooling or reheating for a short time at temperatures of 850°C or lower. Studies of grain boundary hardness vs time of aging showed there was no "overaging" effect.

Several experiments were conducted to learn the effect of time of high temperature soaking at 900°C upon subsequent hardness level. Figure 2 shows the results of heating 52 A/o Ga samples in air at 900°C for various

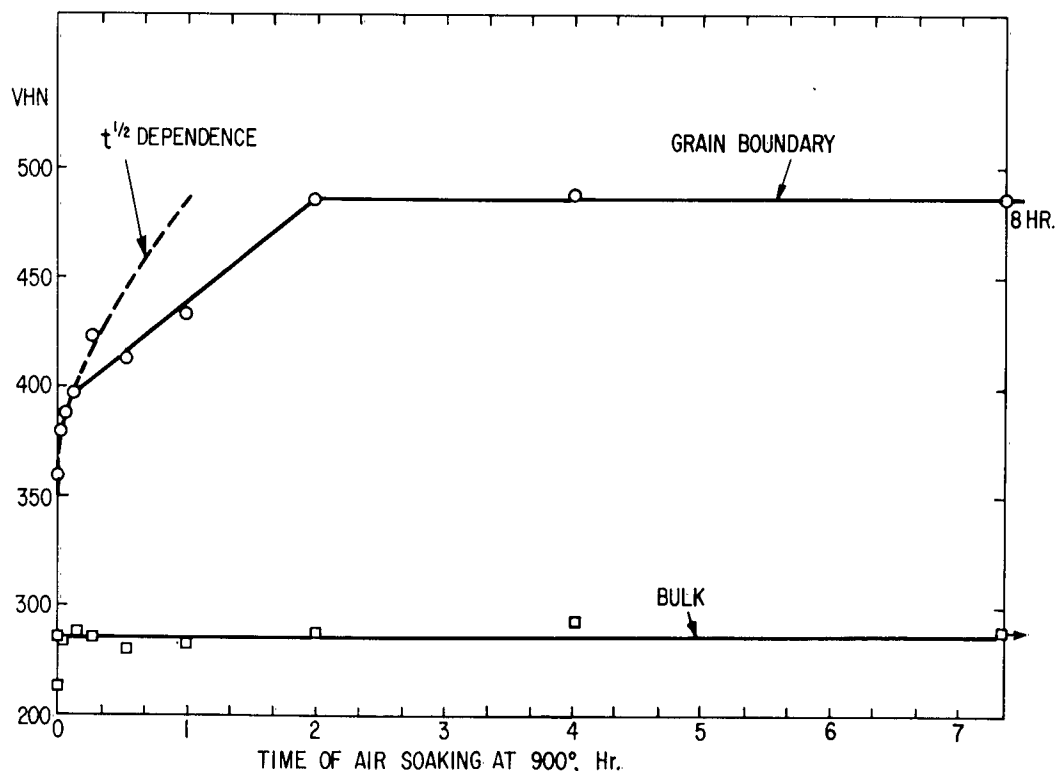


Fig. 2 Hardness of grain and grain boundaries as a function of soaking time at 900°C in air, followed by air cool (52 A/o Ga).

intervals of time followed by air cooling. It has been repeatedly demonstrated that air cooling results in maximum hardness when following an oxygen diffusion heat treatment.

There are three parts in the grain boundary-hardness plot. For the first 10 minutes, the increase in hardness is proportional to the square root of time, as would be expected for a diffusion-controlled reaction. Next, between 10 minutes and 2 hours, the increase in hardness is approximately linear with time until saturation at the surface is reached at about 2 hours and the hardness no longer changes with increased time. The bulk hardness remains at approximately 286 throughout. It must be emphasized that these results apply to measurements made just below the original gas-metal interface. Obviously the first few atom layers of NiGa, while perhaps instantaneously saturated with oxygen, can have no measurable effect upon the hardness. However, as increasing depths from the surface attain some minimum oxygen content a point is reached where the effect is sufficiently pronounced to affect the microhardness. Because the effective "hardness depth" is below the true gas-metal interface, the region of the hardness impressions is subject to a diffusion flux of oxygen moving in along the grain boundary and also perpendicularly from the grain boundary into the bulk alloy. Since a saturation, or final constant hardness, must eventually be reached, one would anticipate a region of changing kinetics between the region of square root of time dependence and the final region of independence of time. Because of the two-directional character of the oxygen diffusion in this system, a precise analysis of the hardness-time dependence does not seem feasible, nor does it appear to be necessary.

After establishing that 900°C was very close to a minimum temperature for "quenching-out" the grain boundary hardening effect, and that 2 hours produced maximum hardening, a more detailed series of experiments was carried out to learn the effect of reheating temperature upon the hardness level. A batch of samples was given a 2-hour 900°C soak in 1 atm of oxygen and quenched rapidly in cold water. Individual samples from this batch were subsequently reheated, usually in a salt bath, and again cold water quenched. The time chosen for each "aging" heat treatment was more than long enough to reach a maximum hardness, although the minimum time to reach this level is short at high temperatures and long at lower temperatures, as would be anticipated for a diffusion-controlled process (see below). In general, these times were at least 10 times those required to reach maximum hardness. These results are shown in Fig. 3, where the figure beside each point represents holding time at temperature in minutes.

It is obvious that the boundary hardness remained at a constant level of about 480 VHN until a temperature somewhat in excess of 875°C was reached. Upon increasing the temperature beyond 875°C, a rapid drop of hardness occurred until at approximately 900°C a constant level close to 300 VHN was obtained; i. e., the grain boundary and bulk hardness were the same.

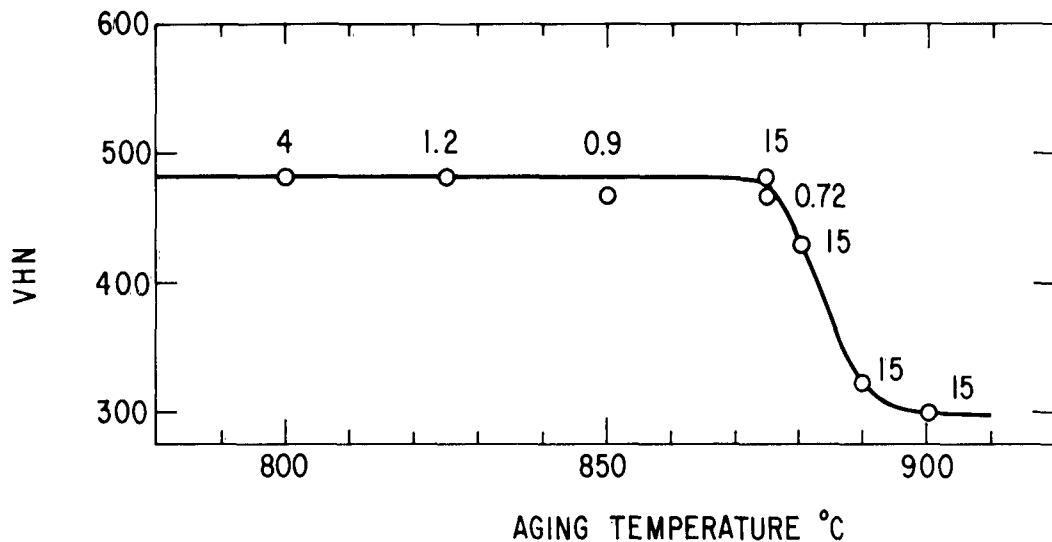


Fig. 3 Hardness of grain boundaries after 2 hours 900°C, O<sub>2</sub>, quenched, then aged at indicated temperatures for periods of time in minutes noted at each point (52 A/o Ga).

The results just cited showed that samples given an oxygen-diffusion heat treatment at 900°C could be softened by quenching at 900°C, but it had not been demonstrated that this quenching treatment was equally effective for specimens exposed at higher temperatures. Also, there was a question if samples exposed to oxygen at lower temperatures could be rendered soft by quenching from lower temperatures.

To settle these questions, two heat treating experiments were performed on hydrogen-cleaned 52 A/o Ga samples. In the first case, a sample was exposed to air at 800°C for four hours and then cold water quenched. The grain boundaries were 338 VHN while the bulk was 302 VHN. Evidently quenching from the oxygen-soaking temperature was not adequate to prevent grain boundary hardening.

In the second experiment, a similar sample was heated to 1000°C in air for 2 hours, and then was furnace cooled to 900°C. When this temperature was reached, the specimen was cold water quenched. Results gave a grain boundary hardness of 296 and a bulk hardness of 295. In this case, although the sample was exposed to air at a higher temperature than the quenching temperature, nevertheless a 900°C quench was sufficient to prevent the hardening reaction.

One can conclude from these experiments that the critical factor in preventing the hardening reaction is not the relative levels of oxygen-exposure

temperature and quenching temperature but rather the absolute level of 900°C for quenching.

#### KINETICS OF THE HARDENING REACTION IN NiGa, 52 A/o Ga

Having established (1) that heating samples for 2 hours in oxygen at 1 atm pressure at 900°C provided ample oxygen contamination for a large hardening effect and (2) that rapid quenching from this temperature suppressed the hardening reaction until later reheating or "aging," it was possible then to proceed to a study of the hardening kinetics.

The "aging" heat treatments for the kinetic study were nearly all done in a salt bath following the oxygen gas charging treatment of 2 hours at 900°C.  $\text{NaNO}_2\text{-KNO}_3$  bath was used for temperatures up to 600°C, and for higher temperatures a commercial chloride-type bath was used. The salt bath heat treatments were convenient both from the standpoint of being chemically inert (no oxygen contamination) and from the standpoint of rapid heating to temperature. This latter feature was particularly important at higher aging temperatures where control of time to within a few seconds was necessary. The regular cold water quenching procedure which followed all salt bath heat treatments not only allowed good control of heat treating time, but it also removed the adherent salt film.

Samples used once could be prepared for reuse by an extended dry hydrogen atmosphere heat treatment at 900°C. It was observed that a 24-hour treatment in hydrogen at this temperature was amply long to erase all previous oxygen contamination. In fact, hydrogen-reduced samples gave exactly the same results as originally observed on virgin material. Several cycles of oxygen charging, aging, and hydrogen deoxidation proved to be feasible. Eventually, however, the repeated quenching stresses caused so much cracking that samples could no longer be reused without going through a melting cycle.

Figure 4 shows a typical hardening curve during aging treatment of an oxygen charged specimen. It is to be noted that the original grain boundary hardness of 300 (same as the bulk) increases to 480 VHN after about 5 minutes, but beyond this time the hardness remains constant. Some samples have been aged at temperatures in this region for over 70 hours without showing any softening tendency. Figure 5 shows the same 700°C data for the period of increasing hardness against the square root of time together with similar results at 500° and 425°C. Since the data plotted in this manner follow a straight line, it appears that the hardening process is diffusion-controlled.

To correlate hardening rate as a function of temperature, some suitable rate constant must be chosen. Several possibilities suggest themselves, such as time to reach maximum hardness, time to reach half hardness, or time to reach a certain hardness level. In actual practice it does not matter

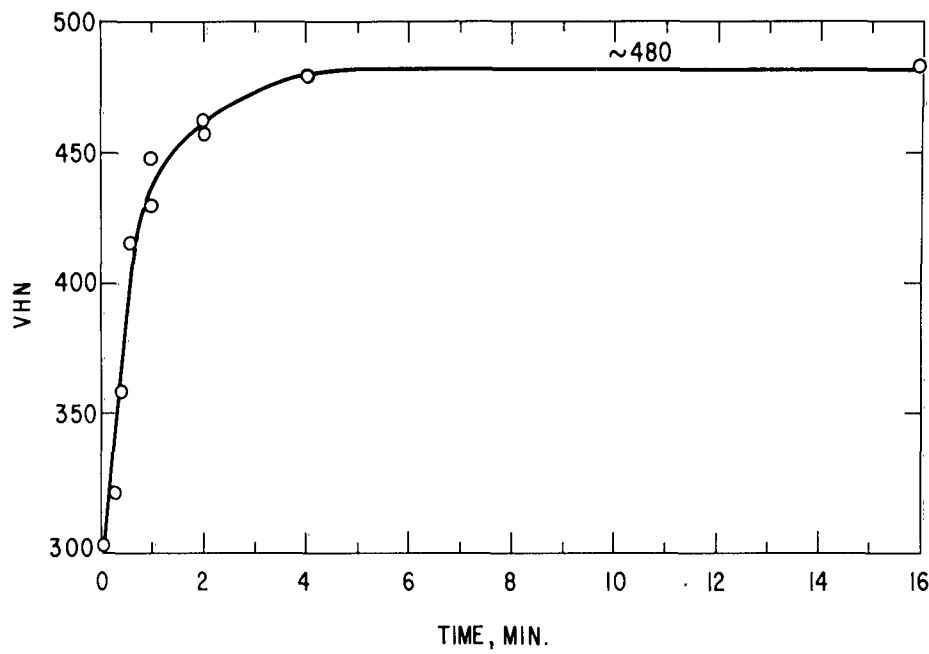


Fig. 4 Rate of hardening at 700°C (52 A/o Ga).

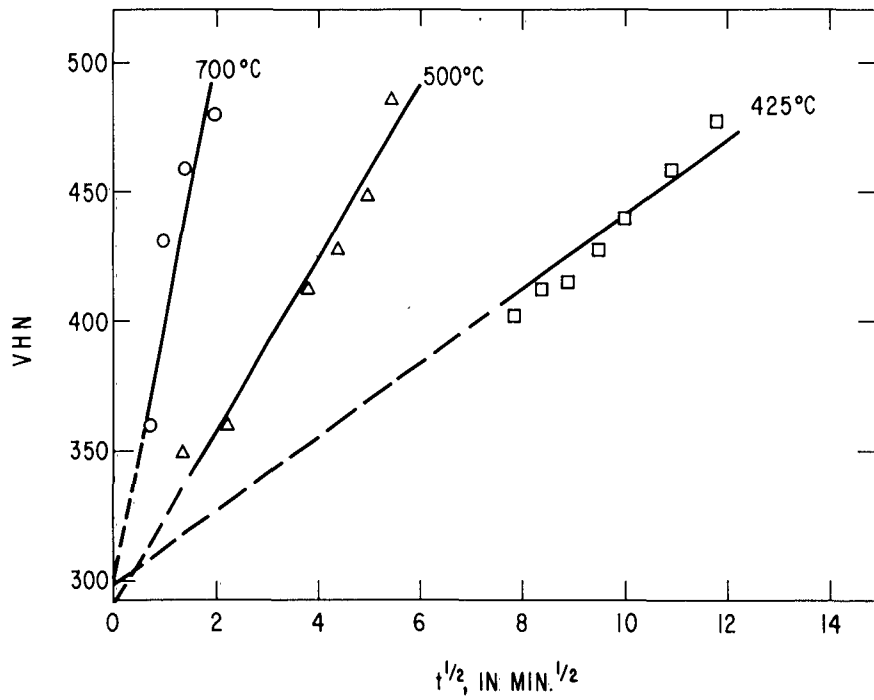


Fig. 5 VHN vs square root of time (52 A/o Ga).

much what criterion is adopted, but it was decided to use time to reach a Vickers Hardness Number (VHN) of 450. The log of this time is plotted against reciprocal temperature in Fig. 6, and the data are given in Table I.

If one replots in terms of maximum hardness, one observes the same relationship; but the scatter is considerably greater, probably because it is not easy to pick out a tangent point to a rather large curve. On the other hand, very frequently the 450 VHN point fell on a part of the curve which appears nearly linear in rectangular coordinates (see Fig. 4).

The data appear to be best treated as three-branched curve representing at least two processes. (If one assumes that a single process is involved and attempts to fit all points to a single line, the scatter becomes much worse.) The high-temperature process has an apparent activation energy of about 57 kcal, while the low-temperature process has an activation energy of about 33 kcal. The intermediate range yields a very low value of something like 9 kcal, and it seems very doubtful if this region corresponds to a single process. Tentatively, it is considered possible that the 57 kcal figure represents the activation energy for gallium volume diffusion. The 33 kcal value might be for gallium diffusion along grain boundaries or diffusion due to some other short-circuiting diffusion process.

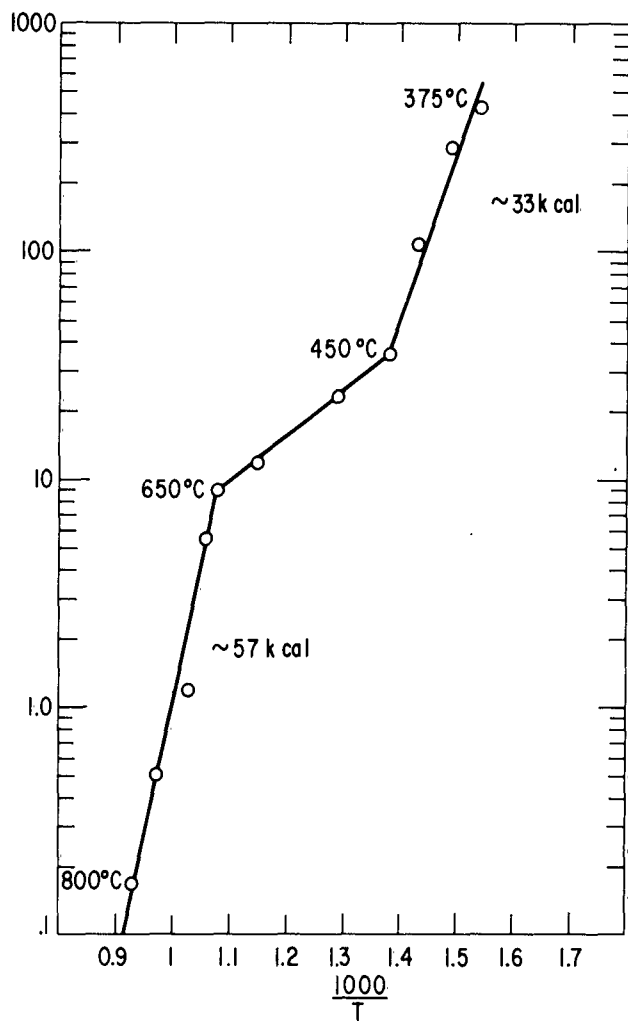


Fig. 6 Time in minutes required to reach 450 VHN as function of temperature (52 A/o Ga).

boundaries or diffusion due to some other short-circuiting diffusion process.

TABLE I

Time Required to Reach VHN = 450 at Various Temperatures

<u>°C</u>	<u>Time (min)</u>
375	426
400	288
425	111
450	36
500	23
600	12
650	9
675	5.5
700	1.2
750	0.50
800	.17

Because of the peculiar shape of the hardening rate/temperature relation shown in Fig. 6, it was decided to make certain that the three-branched behavior was not due to a solid-state transformation in NiGa. To investigate this possibility, the following properties were measured as a function of temperature: dilation, electrical resistivity, and hot hardness. None of these properties showed any significant discontinuities in the property-temperature plot. Finally, "hot x-ray" examination at 500°C and at 700°C showed no new lines as compared to room temperature measurements. Hence it must be concluded that anomalies in the basic structure of NiGa cannot explain any of the heat-treating vagaries observed. Further comment about the kinetic results will be postponed until later.

## OXYGEN PENETRATION STUDIES

Attention so far has been confined to an examination of hardening reactions at, or close to, the gas-alloy interface. To investigate the kind and degree of penetration of oxygen into the structure, a series of coarsely polycrystalline samples was prepared. These were made by melting 52A % Ga alloy in 3/8-inch-diameter fused silica tubes in an argon atmosphere, using the Bridgman technique of gradually lowering the tube through the melting zone. This procedure is ordinarily used for growing single crystals, but in this instance only coarse-grained polycrystals were desired and were usually obtained. These crystal grains were in the range of 2 to 5 mm in diameter. Since the heat flow was along the axis of the frozen rod, the grain boundaries were lined up in this direction. Hence, on cutting transverse

cylindrical disks several millimeters thick, the grain configuration was the same on both flat surfaces, indicating that any element of the grain boundary surface was perpendicular to the cut (flat) surface.

Several samples of this type were heated in oxygen or in air for various periods of time, and were then cut in two along a disk diameter. This newly cut surface exposed in general one grain boundary which extended from one semicircular flat area to the other one, and perpendicular to the gas-alloy interface. Hence, if there existed an oxygen concentration gradient from the gas-alloy interface inward, one would expect higher hardness levels at either end of the grain boundary, falling off inward toward the center of the disk. This is exactly what was observed (see Fig. 7). This coarse-grained sample had been heated in oxygen at 1000°C for 16 1/2 hours, and was then air cooled to allow the hardening reaction to set up. Hardness-distance curves are shown for both the grain boundary and the bulk alloy. In the latter case, measurements were made at least 2 mm away from the grain boundary, so that there would be no chance of picking up any hardening attributable to the grain boundary region. Not only is the surface grain boundary hardness much

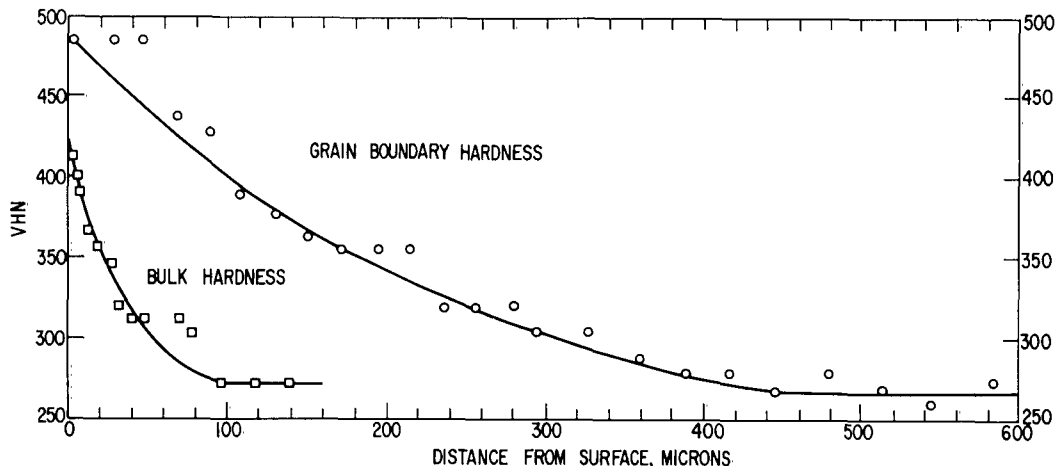


Fig. 7 Grain boundary and bulk hardness as a function of distance from the gas-metal interface. 52 A/o alloy heated at 1000°C for 16 1/2 hours in oxygen.

higher than the bulk, but the depth of penetration of the hardening effect is many times deeper. Since this sample was given a much longer exposure to oxygen at high temperature than the previous standard 2 hours at 900°C, it is not surprising that the bulk hardness at or near the surface is higher than 300. In addition, hardness profiles made in the manner just described generally show higher surface hardness because the surface oxide at the original gas-metal interface is still intact. Similar samples were prepared at the following temperatures, with similar results: 600°, 700°, 800°, 900°C.

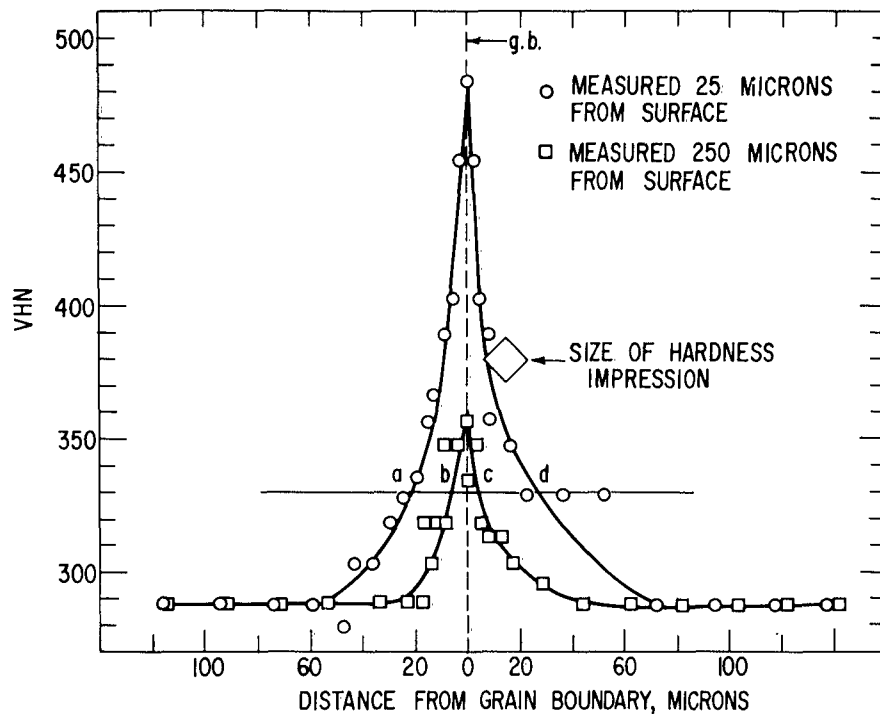


Fig. 8 VHN vs distance from grain boundary at two depths from the gas-metal interface. 52 A/o Ga alloy heated for 4 hours at 900°C in oxygen.

Having demonstrated that samples show a hardness-depth gradient in both grain boundaries and in the bulk, the hardening behavior perpendicular to the grain boundary was examined. An example of typical results is shown in Fig. 8 where a sample prepared as described above had been heated for 4 hours at 900°C in oxygen. Hardness traverses were made across the grain boundary at 25 microns and at 250 microns from the gas-alloy interface. As would be anticipated, the region close to the grain boundary was much harder near the gas-alloy interface, than farther away from it.

While no rigid proof can be offered that these hardness gradients along and transverse to grain boundaries are due to oxygen, this conclusion seems inescapable. It is obvious that there is an oxygen gradient possible along a line perpendicular to the gas-alloy interface, granting some slight oxygen solubility in the alloy. It is almost equally obvious that no other component of the system could have this kind of concentration gradient. Certainly one cannot argue that there is a nickel or a gallium concentration gradient in this direction.

Another kind of experiment was devised to provide additional evidence for the thesis that the observed hardening is a function of the oxygen content. Two coarse-grained NiGa disk samples of the standard 52 A/o Ga alloy were

given superficial oxide films by oxidizing one for 15 minutes at 700°C in air, the other for 1 minute under the same conditions. The latter sample showed a hardly appreciable yellow interference color, while the 15-minute exposure resulted in a light brown film. These two samples were then sealed into fused silica capsules at  $10^{-4}$  mm vacuum and were heated for 4 hours at 900°C to diffuse oxygen inward from the films on the surface. The samples were allowed to air cool to set up the hardening reaction. Finally, just as in the samples discussed above, they were each cut along a disk diameter, and the hardness gradient determined from the surface inward.

Figure 9 shows, as expected, that in the case of the sample with the thicker film, the hardening penetrated appreciably deeper both along grain boundaries and through the bulk. This result seems to provide fairly clear-cut evidence that the hardening is perhaps at least roughly proportional to the amount of oxygen present.

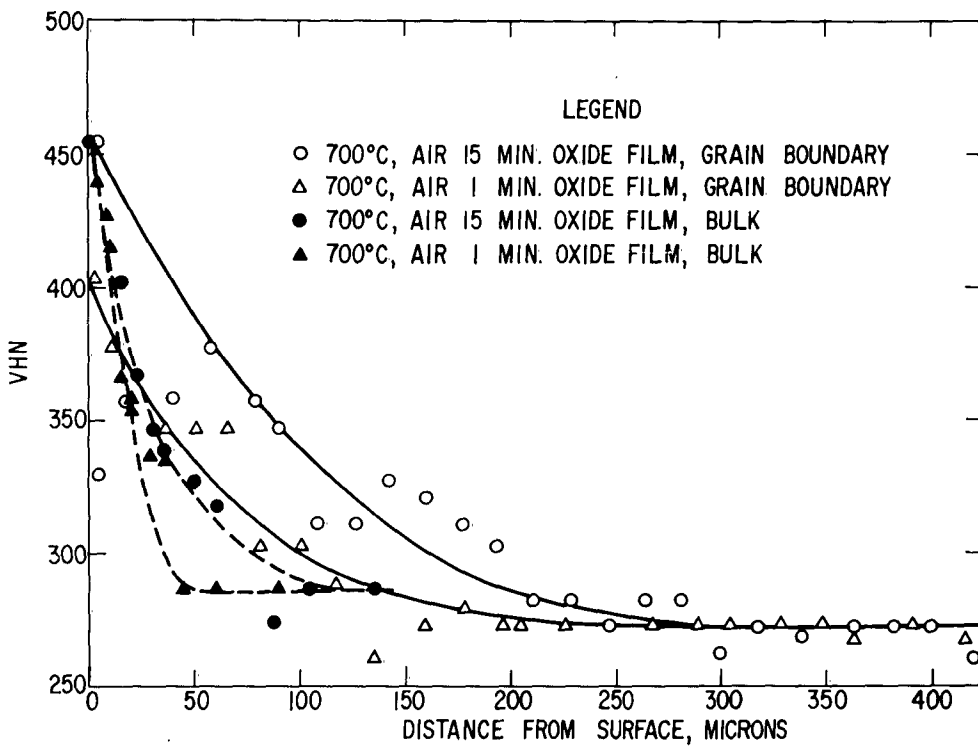


Fig. 9 Hardness contours originating from surface oxide films formed at 700°C, followed by 4 hours 900°C vacuum treatment (52 A/o Ga alloy).

## CALCULATION OF OXYGEN DIFFUSION CONSTANTS

Hardness-distance plots such as that in Fig. 7 have the same shape as a concentration-distance plot obtained from a diffusion experiment. In fact, there is precedent for the determination of diffusion constants from micro-hardness data; see Bueckle, (5) and Sims, Klopp, and Jaffee, (6)

The work of Sims *et al.* (6) is particularly pertinent because they were concerned in estimating the diffusion rate of oxygen in niobium. Their results were later corroborated by the more elegant internal friction technique. An oxygen diffusion analysis is possible if it is assumed that the increase in hardness over the base level is proportional to oxygen concentration. In the absence of any contrary evidence, this assumption appears to be justifiable.

It seems fairly clear from Figs. 7 and 8 that two diffusion constants are involved:  $D$ , the diffusion constant in the bulk and  $D'$ , the diffusion constant along the grain boundary.

LeClaire<sup>(7)</sup> has made an analysis of the ratio of  $D'/D$  in terms of a characteristic angle  $\alpha$  which is determined ordinarily by an isocentration line formed near a grain boundary by a suitable etching solution. That is, the etching solution outlines a zone of a constant composition because of constant chemical reactivity. In the case to be considered here, however, hardness measurements can be used since we are postulating that equal hardness implies equal oxygen concentration. Therefore, in Fig. 8, the points labeled a, b, c, d, are of equal oxygen concentration. Hence by constructing a right triangle whose long side is  $250 - 25 = 225$  microns, and whose short side is half the distance ad-bc, we find the acute angle  $\alpha$ , and hence its cotangent as required in the LeClaire analysis.

LeClaire's expression is

$$\frac{D'}{D} = \frac{1}{5} 2(\pi Dt)^{1/2} \cot^2 \alpha \quad (1)$$

where  $D'$  = grain boundary diffusion constant,  $\text{cm}^2/\text{sec}$

$D$  = bulk diffusion constant,  $\text{cm}^2/\text{sec}$

$\delta$  = thickness of grain boundary, assumed to be  $5 \times 10^{-8} \text{ cm}$

$t$  = time in seconds

$\alpha$  = angle between grain boundary and line of constant composition.

Since  $D$  appears twice in Eq. (1) it is convenient to use the ratio  $D'/D^{3/2}$  which is thus calculated to be  $0.98 \times 10^{12}$  for the situation shown in Fig. 8, 4 hours at  $900^\circ\text{C}$  in oxygen.

Fisher<sup>(8)</sup> has analyzed simultaneous grain boundary and volume diffusion and has since made the suggestion<sup>(9)</sup> that his original expression for the

variation of concentration along and transverse to a grain boundary can be slightly modified to make use of the hardness profile along a grain boundary. Again, the assumption is made that concentration is proportional to hardness.

Fisher's original expression was

$$C = \exp \left( -2^{1/2} y_1 / \pi^{1/4} t_1^{1/4} \right) \operatorname{erfc} \left( x_1 / 2t_1^{1/2} \right) \quad (2)$$

where C is concentration of the diffusion substance

y is distance along boundary

x is distance transverse to boundary

$t_1 = Dt/\delta^2$

t = time in secs

D = bulk diffusion constant

$D'$  = grain boundary diffusion constant

$\delta$  = grain boundary thickness, assumed here, as usual, to be  
 $5 \times 10^{-8}$  cm

$y_1 = y/\delta$   $(D'/D)^{1/2}$

$x_1 = x/\delta$ .

Since in this part of the calculation we are concerned with the concentration profile along the grain boundary (as measured by hardness),  $X = 0$  and hence  $\operatorname{erfc}(0) = \text{constant}$ . Hence the hardness increment over the minimum grain boundary hardness  $H - H_0$  or  $(\Delta H)$  can be expressed as

$$\Delta H = \text{constant} \exp \left( -2y_1^{1/2} / \pi^{1/4} t_1^{1/4} \right) \quad (3)$$

taking logarithms, and substituting expression in y and t for  $y_1$  and  $t_1$ :

$$2.3 \log \Delta H = \text{const} - \frac{2^{1/2}}{\pi^{1/4}} \left( \frac{D'}{D} \right)^{-1/2} \frac{y}{\delta^{1/2} (Dt)^{1/4}}$$

The data desired for a solution for  $D'/D$  is  $\log \Delta H$  as a function of y. Since  $(2.3 d \log \Delta H) / dy$  is the slope of such a plot, the right-hand member of Eq. (4) can be evaluated.

$$\frac{2.3 d(\log \Delta H)}{dy} = - \frac{2^{1/2}}{\pi^{1/4}} \cdot \left( \frac{D'}{D} \right)^{-1/2} \cdot \frac{1}{\delta^{1/2} (Dt)^{1/4}} \quad (4)$$

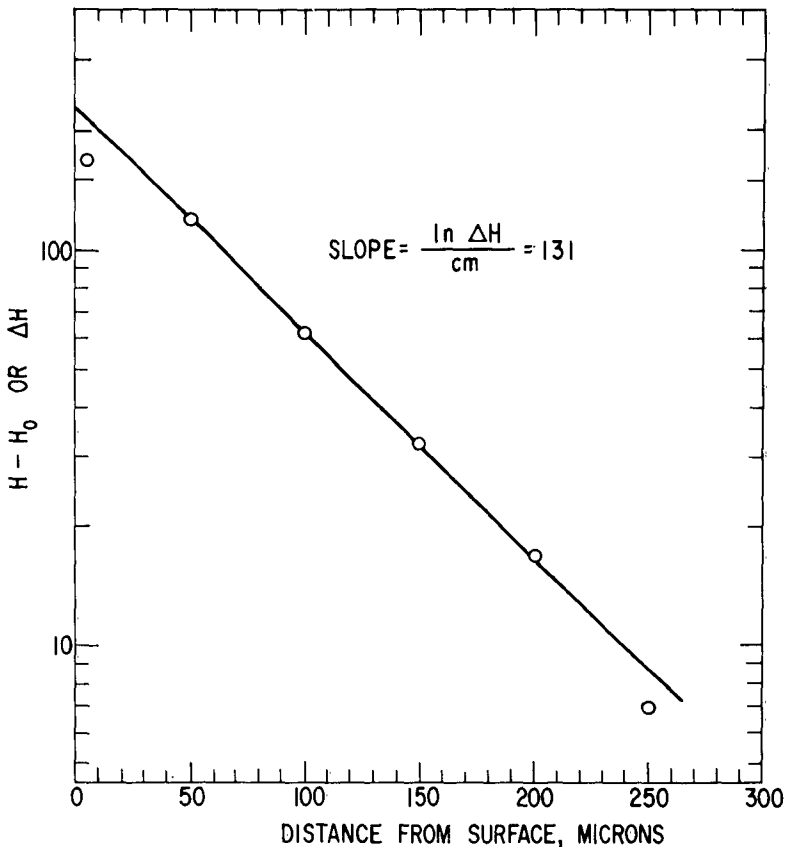


Fig. 10  $\Delta H$  along a grain boundary vs distance from surface.

The experimental data for the coarse-grained 52 A/o Ga-NiGa alloy exposed to 900°C in oxygen for 4 hours are plotted in this manner in Fig. 10. The slope,  $2.3 \log \Delta H/\text{cm}$ , is found to be 131. Since from LeClaire's expression  $D' = 0.98 \times 10^{12} D^{3/2}$ , as already stated, one can now substitute this in Eq. (4) and get a solution for  $D$ .  $D$  is  $1.1 \times 10^{-11} \text{ cm}^2/\text{sec}$  and  $D'$  is  $3.58 \times 10^{-5} \text{ cm}^2/\text{sec}$ . These figures appear to be reasonable ones for oxygen diffusion at 900°C through bulk crystals and along grain boundaries.

When one performs this analysis on each of several coarse grained, 52 A/o Ga alloys which have been heat treated in oxygen or in air, the results shown in Table II are obtained.

Two bulk alloy profiles (see one example in Fig. 7) were analyzed by the standard error function diffusion equation on the assumption that hardness is proportional to oxygen concentration. The concentration function used was

$$\frac{H - H_0}{2(H_m - H_0)}$$

where

$H$  = hardness number at any distance from the gas-metal interface  
 $H_0$  = minimum hardness  
 $H_m$  = maximum (surface) hardness

The fraction is plotted vs distance  $y$ , and a best fit on probability paper obtained, where

$$\frac{H - H_0}{2(H_m - H_0)} = 0.5 \text{ at } y = 0.$$

TABLE II

Bulk D, and Grain Boundary D', Diffusion Constants after Various Heat Treatments in Oxygen or Air, 52 A/o Ga Alloy

°C	Time (hr)	D (cm <sup>2</sup> /sec)	D' (cm <sup>2</sup> /sec)	D from Bulk Conc. Gradient (cm <sup>2</sup> /sec)
		5.43 x 10 <sup>-13</sup>	3.5 x 10 <sup>-6</sup>	1 x 10 <sup>-11</sup>
600	24	2.7 x 10 <sup>-12</sup>	3.87 x 10 <sup>-5</sup>	--
700	24	1.58 x 10 <sup>-12</sup>	1.42 x 10 <sup>-5</sup>	6 x 10 <sup>-11</sup>
800	16	1.1 x 10 <sup>-11</sup>	3.58 x 10 <sup>-5</sup>	--
900	4	1.4 x 10 <sup>-12</sup>	2.95 x 10 <sup>-5</sup>	6 x 10 <sup>-11</sup>

It will be noted that the oxygen diffusion constant obtained in this manner is appreciably larger than that calculated by the LeClaire-Fisher analysis. However, considering the scatter of the hardness data, and the assumptions implicit in the analytical separation of D from D' in the case of grain boundary diffusion, this is perhaps satisfactory agreement.

The scatter in D and D' as a function of temperature is disappointing, but again one perhaps could not expect better results from hardness data, with their inherent high scatter due to local inhomogeneities, impurity effects, mechanical vibration of the hardness tester, etc. It might be suggested that since there is very little trend in D with temperature, the activation energy associated with the movement of oxygen through the NiGa lattice is low.

#### STABILITY OF THE HARDENING REACTION

No information as yet had been obtained on the stability of the hardness contour after long exposure at temperatures in the "solution-treating" range of 900°C or above.

There are two kinds of heat treatment which can cause grain boundary and bulk softening, as measured at room temperature. One is heating at a

sufficiently high temperature followed by rapid quenching. The other is heating at a sufficiently high temperature in the absence of oxygen contamination. In the first type of heat treatment, the duration of the heat treatment must be sufficiently long to cause (presumably) enough diffusion away from regions where concentration of hardening solutes had caused both grain boundary and bulk hardening. This point is illustrated in Fig. 11 which shows the hardness distribution with distance using the same kind of sample described for the diffusion experiments. It will be noted that the grain boundary hardening after an initial exposure to oxygen at 900°C for 2 hours and slow cooling persists inward to about 600 microns, while the bulk hardening extends to about 80 microns. After an additional exposure in air at 900°C for 1 hour followed by a cold water quench, the grain boundary hardening extends to only about 30 microns while the bulk hardening is somewhat deeper at approximately 40 microns. The deeper hardening contour of the bulk sample after this treatment would be expected on the basis of more rapid diffusion along grain boundaries as compared to diffusion through the bulk. The surface hardness in both cases has been considerably reduced. However, the hardness contour is not yet flat. To give the sample a more drastic diffusion heat treatment, a duplicate sample which was still in the 2-hour 900°C oxygen soak, slow cool, condition was heated in air at 950°C for 4 hours and then rapidly water quenched. This time both grain boundaries and bulk were down to the same low value of about 270 VHN. It is perhaps possible that the minimum quenching temperature is somewhat a function of oxygen concentration, and that layers close to the surface require a slightly higher temperature to quench-out the hardening reaction. At the present time it is not certain whether the somewhat higher temperature (950°C) or the more extreme diffusion heat treatment was of primary importance.

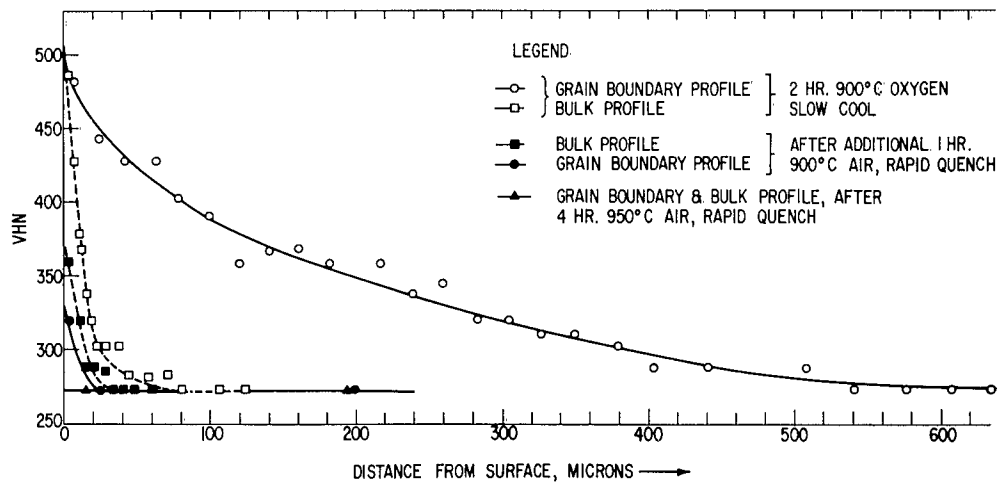


Fig. 11 Effect of heat treatments on the hardness contour of a sample heated to 900°C, O<sub>2</sub> for 2 hours.

A drastic quench to obtain softening is not necessary if the oxygen concentration gradient is leveled by a heat treatment in an atmosphere containing no oxygen. To illustrate this point, a 52 A/o Ga coarse-grained sample of the type just described in the previous experiment was given a 2-hour soak in air at 900°C followed by an air cool. From other experiments it was known that the hardness gradient from the surface inward along the grain boundary, and through the bulk, was as shown in Fig. 11. The sample was surface cleaned by an acid etching solution to remove surface oxide. However, traces of surface oxide formed by air attack at room temperature were undoubtedly present. This sample was sealed in a fused silica tube, the sample itself lying in an  $\text{Al}_2\text{O}_3$  crucible. In an adjacent  $\text{Al}_2\text{O}_3$  crucible were several grams of zirconium foil to getter residual gas. The capsule was sealed off at  $10^{-6}$  mm pressure and soaked at 1000°C for 64 hours, after which it was air cooled to room temperature. This cooling rate was sufficiently slow to allow maximum surface hardening to develop in the presence of the oxygen concentration gradient as encapsulated.

However, microhardness exploration now showed a surface hardness in the vicinity of about 290 VHN, dropping off to a value of 270 VHN at about 20 microns from the surface. This slight surface hardening can be attributed to a small oxygen partial pressure diffusing in through the fused silica wall at 1000°C. This seems not unreasonable when we consider that the dissociation pressure of  $\text{Ga}_2\text{O}_3$  at 1000°C is about  $10^{-18}$  atm.

The interpretation of this result is different from that of the experiments cited previously. In this case, no hardening was present because the oxygen concentration at the surface was largely removed by diffusion inward. In the quenching experiments, the oxygen concentration was still high at the surface (both at the grain boundaries and in the bulk), but rapid cooling evidently prevented the high oxygen content from reacting with other components of the system to cause the hardening reaction. This subject will be expanded later on.

To provide additional experimental evidence that a homogenization anneal in a comparatively oxygen-free atmosphere can eliminate the hardening reaction, even when the cooling rate from the anneal is slow, another similar capsule experiment was made. This time the same alloy was heated at 800°C for 4 hours in air for an initial oxygen diffusion heat treatment. After cleaning, this sample was encapsulated as before with a zirconium getter and heated for 24 hours at 900°C and slow (air) cooled.

In this instance, the top surface of the sample at a grain boundary was 311 VHN, while the bulk was 295. However, the underside of the same sample, which had faced the  $\text{Al}_2\text{O}_3$  crucible during the 900°C heat treatment, showed a hardness of 283 at both grain boundaries and at the grain centers. As in the first capsule experiment, some oxygen contamination of the top surface had occurred, but the bottom surface was better shielded. Again the

conclusion is that in the absence of an oxygen-containing atmosphere, a high temperature heat treatment will remove the oxygen-induced hardening, presumably by allowing the oxygen to diffuse to the interior of the sample.

#### METALLOGRAPHY

Figure 12 shows a typical photomicrograph of a 52 A/o Ga alloy in the hardened state, in which the grain boundaries are about 480 VHN and the bulk about 300 VHN. While some grain boundaries are etched more deeply than others, there is no evidence of any second phase at 1000X. Electron microscopy of replicas prepared from similarly appearing hardened samples has not shown any sign of a second phase.

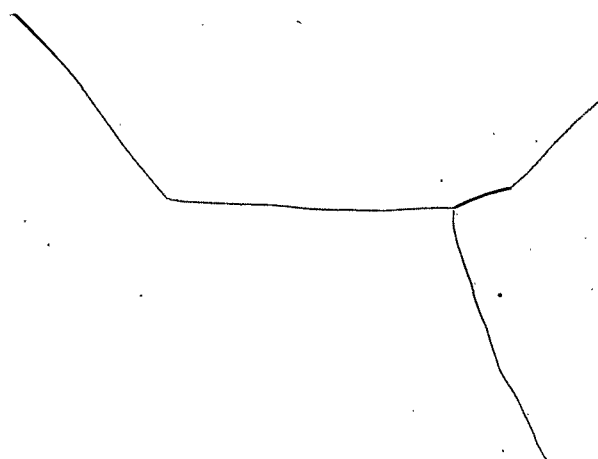


Fig. 12 52 A/o Ga in hardened state, etched HCl + CrO<sub>3</sub>. 1000X

#### DEFECT STRUCTURE OF NiGa

Because the defect structure of crystalline solids is so important to an understanding of solid-state processes, such as transport mechanisms, diffusion rates, etc., it seemed desirable to learn something of the defect structure of NiGa. Such a knowledge might aid in understanding the hardening mechanism, for example, including the effect of stoichiometry on the hardening tendency.

The usual method to study the defect structure is by means of measuring lattice parameter and density as a function of composition. Then, one can calculate theoretical densities assuming certain structural models and compare these calculated densities with the experimental densities. The obvious model to use here is that of NiAl whose defect structure has been established by Bradley and Taylor.<sup>(10)</sup> One can picture the ordered body-centered cubic CsCl structure as composed of two kinds of sites: Ni sites

and Al sites. At the stoichiometric composition for every 100 atoms, 50 atoms are in Ni sites (as at cube corners) and 50 are in Al sites (as at cube centers). At less than 50 A/o Al, the excess Ni atoms go into Al sites. However, beyond 50 A/o Al, Ni atoms are removed from nickel sites, thus creating vacant sites. In other words, up to 50 A/o Al, all sites are filled, but beyond 50 A/o Al, each 1 A/o Al creates 1 per cent vacant Ni sites.

Knowing the size of the unit cell by lattice parameter measurements, one can then calculate what the density of the NiGa phase should be as a function of concentration assuming either (1) all sites filled at all compositions or (2) the NiAl defect structure. Table III gives the data for both experimentally measured lattice parameters and densities, and densities calculated from the above two models. The data are shown graphically in Fig. 13. It can be seen at once that the experimental density curve lies closely parallel to the NiAl defect structure model, hence strongly suggesting that NiGa probably has the same defect structure as NiAl. The absolute discrepancy between the two curves is less than 1 per cent and is in the right direction to be accounted for by some porosity in the cast NiGa samples.

TABLE III  
Lattice Parameters and Densities of NiGa as a Function of Composition

Spec. No.	Ga Nominal (A/o)	Analysis (at. % Ga)	Analysis (wt % Ga)	$a_0$	Exptl. Density	Calc. Density g/cc (all sites filled)	Calc. Density g/cc (of NiAl type)	Molar V(cc)
1675	49	48.6	52.8	2.8952	8.65	8.77	8.77	14.61
1676	50	49.6	53.8	2.8949	8.66	8.82	8.82	14.60
1848	50.7	51.3	55.1	2.8919	8.53	8.85	8.63	14.56
1520	52	51.6	55.7	2.8898	8.40	8.87	8.61	14.52
1849	53	53.7	58.1	2.8828	8.23	8.98	8.33	14.42

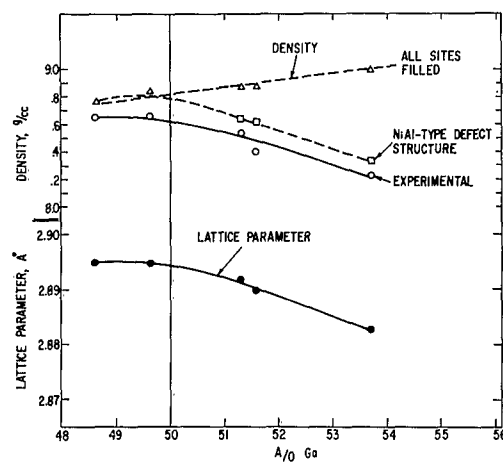
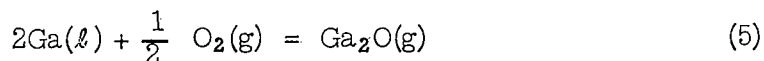


Fig. 13 Density and lattice parameter of NiGa vs composition.

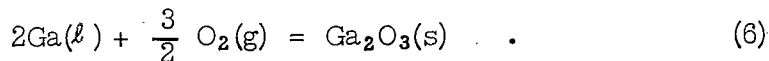
## THERMODYNAMICS OF THE GALLIUM OXIDES

While the thermodynamic properties of  $\text{Ga}_2\text{O}_3$  have apparently been fairly well established for some time, there has been some confusion regarding  $\text{Ga}_2\text{O}$ , the suboxide. For example, Coughlin's(11) tables list  $\text{Ga}_2\text{O}$  as a solid only, while more recent data indicate that at temperatures above 700°K, at least, its normal state is a gas. Glassner's(12) data show it as a solid up to about 1000°K or somewhat lower, then as a gas whose free energy of formation is constant from 1000° to 2500°K, at the -55 kcal level.

Recently, Cochran and Foster(13) studied reactions in systems involving gallium metal vapor,  $\text{Ga}_2\text{O}$  and other stable oxides such as  $\text{SiO}_2$ ,  $\text{MgO}$ ,  $\text{Al}_2\text{O}_3$  and the like. In their paper they listed free energy functions for  $\text{Ga}_2\text{O}_3(\text{s})$  and  $\text{Ga}_2\text{O}(\text{g})$ . Combining these functions with similar ones published by Stull and Sinke(14) for  $\text{Ga}(\ell)$  and  $\text{O}_2(\text{g})$ , one can calculate the free energy of the following two reactions as a function of temperature:



and

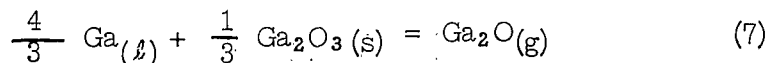


The results are plotted in Fig. 14 for  $\Delta F^\circ_{\text{Ga}_2\text{O}}$  and  $\Delta F^\circ_{\text{Ga}_2\text{O}_3}$  so

3

that each compound is put on a basis of equal oxygen content. The results for  $\text{Ga}_2\text{O}_3$  agree quite closely with the older (1954) tables of Coughlin.(11) However, the data for  $\text{Ga}_2\text{O}(\text{g})$  are apparently new and at least have the appearance of credibility. For example, the positive slope  $\Delta F^\circ$  vs T for  $\text{Ga}_2\text{O}(\text{g})$  seems correct since a gaseous product of higher entropy is being formed. It is particularly of interest to note that the free energy of formation per atom of oxygen of  $\text{Ga}_2\text{O}_3$  is considerably more negative than  $\text{Ga}_2\text{O}$  in the temperature region of interest in this work; 1000°C and below.

Frasch and Thurmond(15) in a recent paper examined the reaction



and measured the vapor pressure of  $\text{Ga}_2\text{O}(\text{g})$  over the temperature range 1073° to 1273°K. This is the temperature range of interest in this work. Over this temperature range the pressure of  $\text{Ga}_2\text{O}$  varied from  $1.56 \times 10^{-4}$  atm to  $9.90 \times 10^{-3}$  atm, respectively. If one calculates the standard free energy of this reaction from these data one obtains +1490 cal/mol at 1200°K while by combination of the two equations given previously one obtains +1400 cal/mol-- excellent agreement.

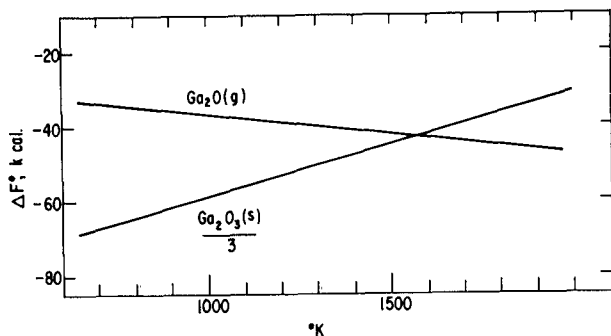


Fig. 14 Free energy of formation of  $\text{Ga}_2\text{O}$  and  $\text{Ga}_2\text{O}_3$  per gram atom of oxygen as a function of temperature.

Although the free energy of this reaction at or near  $1200^\circ\text{K}$  is positive, the positive value is not high. Hence, it is possible to have a small but quite significant pressure of  $\text{Ga}_2\text{O}$ , even though  $\text{Ga}_2\text{O}$  would not be stable if reaction (5) were the only possible source of  $\text{Ga}_2\text{O}$ .

Since  $\text{Ga}_2\text{O}$  is a gas, in a nonisothermal enclosure it will condense in cold parts of the system and possibly disproportionate back to Ga and  $\text{Ga}_2\text{O}_3$ . Hence its formation tends to remove  $\text{Ga}_2\text{O}_3$  from the hot zone as  $\text{Ga}_2\text{O}$ . In the experiments made during the course of this work, there was not much evidence for reaction (7) except in cases where the oxygen pressure in the system was very low, or where wet hydrogen was used as an oxidizing medium. Even in cases where purified argon was used over  $\text{Ga} + \text{Ga}_2\text{O}_3$ , or gallium alloy +  $\text{Ga}_2\text{O}_3$ , the transport rate of gallium as  $\text{Ga}_2\text{O}$  to cold parts of the system appeared to be quite low. More important, however, as will be discussed subsequently, since oxygen gas is not involved in forming  $\text{Ga}_2\text{O}$ , the presence of  $\text{Ga}_2\text{O}$  causes no ambiguity in the equilibrium oxygen pressure over mixtures of  $\text{Ga}_2\text{O}_3$  and Ga or NiGa.

The fact that little or no evidence of  $\text{Ga}_2\text{O}$  was observed in a highly oxidizing atmosphere, such as air, is probably due to the following reaction:



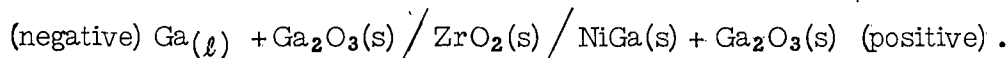
The free energy for this reaction can be readily obtained from the curves of Fig. 14, and it is obvious by inspection that the reaction would proceed to the right, as long as the temperature was not over  $1550^\circ\text{K}$ .

#### ACTIVITY OF GALLIUM IN NiGa

In an alloy where one component is reacting preferentially with the surroundings, the tendency toward that reaction is largely determined by the activity of that component. Hence, if gallium is reacting to form  $\text{Ga}_2\text{O}_3$  from the NiGa alloy, with nickel behaving in an essentially inert manner, one is

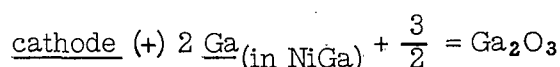
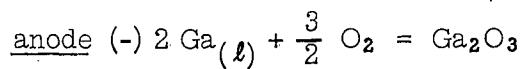
interested primarily in the gallium activity. If a complete knowledge of the gallium activity were available across the composition limits of the NiGa phase, a better understanding might be had of the effect of stoichiometry on the oxygen hardening reaction.

At the suggestion of Wagner, (16) a galvanic cell of the following type was prepared:



This is a solid state cell where one electrode is a mixture of pure liquid gallium + solid  $\text{Ga}_2\text{O}_3$  and the other electrode is a mixture of NiGa alloy of some desired composition also mixed with  $\text{Ga}_2\text{O}_3$ . The  $\text{ZrO}_2$  (CaO-stabilized by about 14 mol/o CaO) acts as the electrolyte since  $\text{ZrO}_2$  is an oxide with anion vacancies and conducts only oxygen anions. It is almost a pure ionic conductor. Since the equilibrium oxygen pressure over  $\text{NiGa} + \text{Ga}_2\text{O}_3$  is higher than that over  $\text{Ga}(\ell) + \text{Ga}_2\text{O}_3$  due to the lowered activity of gallium in NiGa, there is a tendency for oxygen anions to pass from right to left as the cell is written above. There is a counter tendency for cations to move in the opposite direction toward the NiGa electrode (which is positive), but this transfer does not actually happen since  $\text{ZrO}_2$  passes only anions. In actual practice, there is only a very small movement of anions, since the cell is not allowed to deliver power, but is measured in a reversible manner by a d-c potentiometer, which balances the cell's emf.

The electrode reactions can be written:



subtracting,  $\text{Ga}(\ell) = \text{Ga(in NiGa)}$ , which is merely a statement of equilibrium between  $\text{Ga}(\ell)$  and  $\text{Ga}$  in NiGa. From the mass law  $K = a_{\text{Ga}}$ , if the standard state is taken to be pure liquid gallium where  $a_{\text{Ga}} = 1$ . Since we are concerned only with a single component,  $\Delta F$  of the above reaction is actually a partial molal free energy where  $\Delta F = RT \ln a$  and for a galvanic cell  $\Delta \bar{F} = - NFE$  where  $N = \text{valence of ion of interest (oxygen)} = 2$

$F^*$  = Faraday constant = 23,070 cal/volt

$E$  = measured emf in volts.

Physically, the cell as it finally evolved was as sketched in Fig. 15.

Several alloys were examined across the single-phase region including two alloys that were intended to be two-phase alloys at about  $800^\circ\text{C}$ , on either

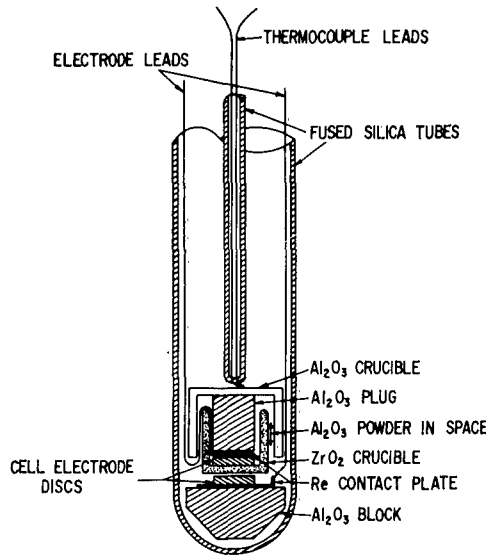


Fig. 15 Solid electrolyte galvanic cell.

was considered to be evidence that equilibrium was probably reached, but a value was not accepted unless a temperature excursion of 835° to 950°C and return reproduced the same result at 835°C. A run usually lasted 2 to 3 days, and the reading in the morning was usually fairly close to that of the preceding evening, within about 5 mv.

The alloys used contained the following atom per cent gallium contents: 41, 49.6, 51.6, 53.7, 57. The three intermediate compositions were analyzed, but the extreme alloys were not. As mentioned earlier, these are two-phase alloys, at least at lower temperatures, and this was confirmed by metallographic examination. Reference to the NiGa phase diagram of Hansen<sup>(4)</sup> shows that at 41 A/o Ga and 835°C, NiGa phase has a composition of about 42 A/o Ga, because the 41 A/o alloy appears to be a two-phase alloy. However, at 950°C, this alloy is single-phase NiGa. At the other composition extreme of the NiGa phase, the 57 A/o alloy is a single phase at both 835° and 950°C.

At 835°C, both extreme compositions lie quite close to the NiGa boundaries, while at 950°C the compositions lie a few per cent within the phase boundaries. For the present purpose, the precise position of the extreme alloys with respect to the phase boundaries is not particularly important, as long as the extreme compositions may be considered to approximate the compositional range of NiGa.

Experiments were made using several alloys against pure gallium, and by using one alloy against another. This allowed a check on internal

-28-

consistency, and a comparison of the relative partial molal free energy of gallium derived from two different routes.

Table IV summarizes the data obtained from the cells: the emf values which were measured directly, and the free energy change derived from their values. Cell 3 means the following cell:

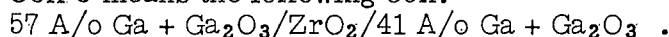


TABLE IV  
Electromotive Force (emf) of the Cells, and Free Energy of Cell Reactions

<u>Cell</u>	<u>emf</u> (mv)	<u><math>\Delta F</math> Cell</u> (cal/mol Ga)
(1) 41 A/o Ga vs Ga		
835°C	157	-7250
950°C	168	-7777
(2) 57 A/o Ga vs Ga		Calculation of $\Delta F_2$ from (1) and (3)
835°C	37	-1710    -1570 $\Delta(\Delta F) = 140$
950°C	36	-1665    -1447 $\Delta(\Delta F) = 218$
(3) 41 A/o Ga vs 57 A/o Ga		
835°C	123	-5680
950°C	137	-6330
(4) 41 A/o Ga vs 49.6 A/o Ga		
835°C	5	-231
950°C	23	-1063
(5) 41 A/o Ga vs 51.6 A/o Ga		
835°C	55	-2540
950°C	63	-2990
(6) 41 A/o Ga vs 53.7 A/o Ga		
835°C	62	-2870
950°C	76	-3510
(7) 53.7 A/o Ga vs Ga		Calculation of $\Delta F_7$ from (1) and (6)
835°C	80	-3700    -4380 $\Delta(\Delta F) = 680$
950°C	73	-3380    -4267 $\Delta(\Delta F) = 887$

The third column gives the free energy change for the cell as written. Hence, cell 3 gives the free energy obtained in reversibly transferring one mole of

gallium from an alloy of 57 A/o Ga to that of 41 A/o Ga where the quantities of each alloy are sufficiently large so that no detectable concentration difference results in either alloy. Cells 1 and 2 give directly the partial molal free energy of gallium in the 41 A/o Ga alloy and in the 57 A/o Ga alloy, respectively, referred to pure liquid gallium. By subtracting from the  $\Delta F$  at 835° and 950°C of cell 1 the corresponding  $\Delta F$  values of cells 3, 4, 5, and 6, relative partial molal free energies of each alloy, referred to liquid gallium, may be obtained. These figures are listed in Table V in columns 2 and 3, along with the activities of gallium calculated from the  $\Delta F_{Ga}$  values according to the relationship

$$\overline{\Delta F}_{Ga} = RT \ln a_{Ga}$$

TABLE V

Partial Molal Free Energy of Gallium Relative to Pure Liquid Gallium,  
and Gallium Activity, at Several Compositions

A/o Ga	$\overline{\Delta F}_{Ga}$ (835°C)	$\overline{\Delta F}_{Ga}$ (950°C)	$a_{Ga}$ (835°C)	$a_{Ga}$ (950°C)	How Obtained
41	-7250	-7777	0.037	0.041	41 vs Ga
49.6	-7019	-6714	.042	.080	41 vs 49.6
51.6	-4710	-4787	.118	.140	41 vs 51.6
[ 53.7	-4380	-4267	.137	.172	41 vs 53.7
53.7 ]	<u>-3700</u>	<u>-3380</u>	<u>.186</u>	<u>.249</u>	53.7 vs Ga
[ 57	<u>-1710</u>	<u>-1665</u>	<u>.460</u>	<u>.504</u>	57 vs Ga
57 ]	-1570	-1447	.491	.552	41 vs 57

The activities are plotted in Fig. 16 against mole fraction Ga x 100 (at. per cent Ga). The filled circles and squares refer to measurements made on alloys which were measured with pure liquid gallium as the other electrode. Hence, these values are more directly obtained and preferred values, as opposed to the open points obtained in a less direct manner. This applies also to Fig. 17, where the relative partial molal free energies are plotted. The preferred values are underlined in Table V. It will be noted at once that the activity changes comparatively little from about 41 to 50 A/o Ga, but that above this concentration the activity increases sharply. At 835°C the activity of the 51.6 A/o Ga alloy used for much of the experimental work, has increased by a factor of three compared to a concentration near the gallium-poor phase boundary.

The kind of relationship between A/o Ga and gallium activity shown in Fig. 16 was previously observed by Kachi<sup>(17)</sup> and by Trzebiatowski and

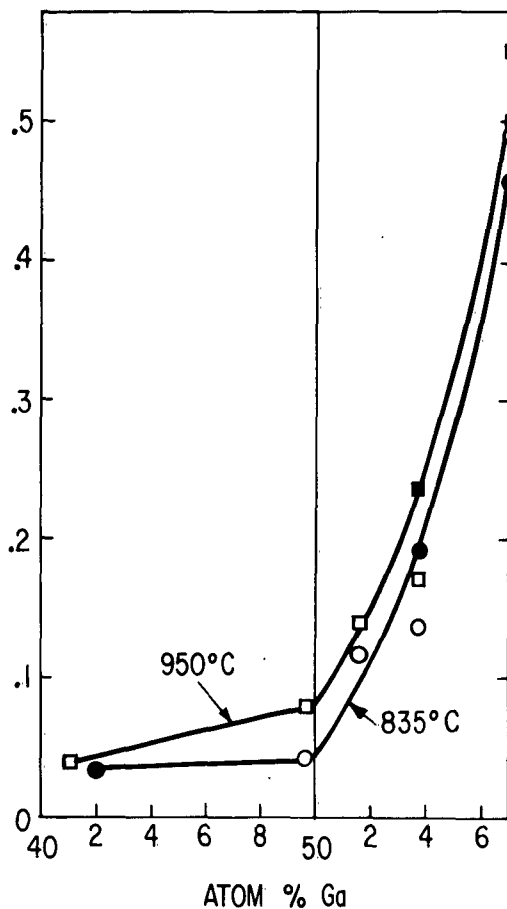


Fig. 16 Activity of gallium in NiGa as a function of composition.

that both the activity and the closely related partial molal free energy are changing very rapidly with composition. It is possible that these observed variations are due to slight inhomogeneities or compositional differences in the alloy powder used to make the electrodes.

In summary, it has been observed that there are sharp changes in the relative partial molal free energy of gallium, and hence in gallium activity, with increasing gallium commencing at 50 A/o Ga. This behavior is undoubtedly significant with respect to the observed effect of stoichiometry upon the oxygen-hardening effect.

Terpilowski(18) in the case of magnesium in AgMg, another intermetallic compound of CsCl structure. Westbrook and Wood(2, 3) have studied this compound intensively and as mentioned early in this report, they found pronounced grain-boundary hardening in AgMg which had been heated in oxygen or in air. It is interesting that the magnesium activity across the phase field of AgMg at 500°C changed by a factor of 12, about the same as observed for NiGa at 835°C (homologous temperatures of about 0.71 and 0.83, respectively).

Another way of showing a significant discontinuity in the thermodynamic properties with composition is to plot the  $\Delta F_{\text{Ga}}$  values against A/o Ga. Figure 17 shows such a plot, where a dramatic change in  $\Delta F_{\text{Ga}}$  occurs just beyond the 50 A/o Ga composition.

It will be noted in Table V that while the free energy discrepancy for the 57 A/o Ga alloy observed directly and indirectly is fairly small, there is a larger difference at 53.7 A/o Ga. The reason for the larger variation for the last alloy is not clear. However, it is obvious from both Figs. 16 and 17

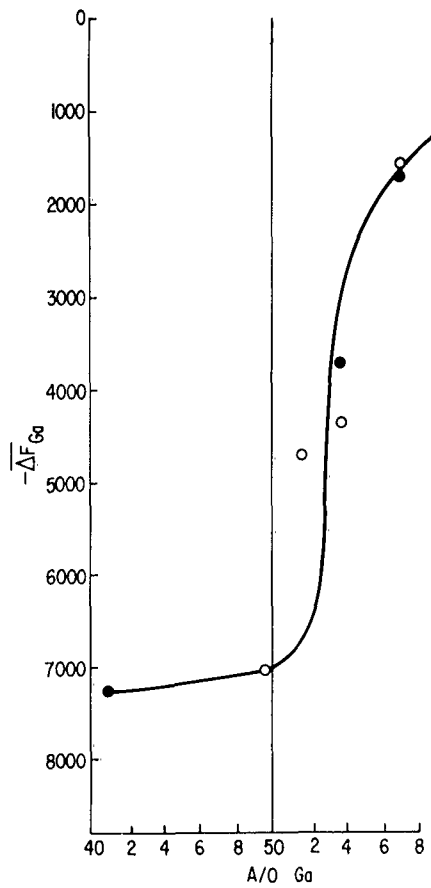


Fig. 17 Partial molal free energy of gallium in NiGa at 835°C as a function of composition.

#### EFFECT OF OXYGEN ON NiGa STRUCTURES

A considerable effort was made to use electron transmission microscopy to obtain some additional insight into the hardening mechanism. It was thought possible that a low-oxygen NiGa sample, or one which after oxygen exposure had been rapidly quenched from 900°C or above, would perhaps show a relatively simple grain-boundary structure. However, a sample which was grain boundary hard might be expected to show a precipitate, or Preston-Guinier zones, or some structural features at the grain boundaries.

Samples of 52 A/o Ga NiGa were first ground down to 3-mil foil by hand lapping on a block, and electrolytic jet impingement was then used to thin down the material for electron transmission. However, the material did not thin in a uniform manner, but rather tended to form many holes through the section. These holes enlarged upon further etching without causing adequate thinning adjacent to the holes. Also, the grain boundaries, even in the

as-cast (oxygen-free) material, tended to be very brittle to the extent that samples would crack up into small fragments during the electrolytic thinning. Two different electrolytic solutions yielded about the same unsatisfactory results. Until some new procedure can be found, it seemed necessary to abandon thinning sections for electron microscopy.

As another approach to the problem, attempts were made to prepare NiGa films by sputtering and by evaporation techniques. Neither of these procedures yielded a satisfactory structure. Sputtering of NiGa merely created an agglomeration of particles which showed no recognizable grain boundaries. Evaporation of pure gallium allowed the gallium to ball up into droplets due to surface tension forces whether the substrate of nickel was hot or cold.

Electron diffraction examination of a fractured grain-boundary surface showed some diffraction spots which could not be identified. However, even if the diffracting substance could be identified, there would still be a question whether this substance had any relation to the hardening complex.

Three 52 A/o Ga samples were examined for possible changes in lattice parameter due to oxygen going into solution. These samples had all been hydrogen-treated at 900°C for 24 hours, slow cool, prior to use. One was set aside as a comparison sample, and the other two were soaked in air at 900°C for 1 hour and 16 hours, respectively, followed by a rapid cold water quench. These samples were small pieces about 3/16 inch in diameter and about 0.060 inch thick. The purpose of the rapid quench was to keep oxygen in solution.

The lattice parameters of these samples, after a standard electro-polish to remove surface strains, were measured by back-reflection x-ray diffraction. The results are shown below.

Sample No.	Treatment	$a_0$ [ $\pm 0.0002$ ]	$\Delta a_0$
1966	As H <sub>2</sub> -treated	2.8897	--
1968	1 hr 900°C, air q.	2.8861	-0.0036
1967	16 hr 900°C, air q.	2.8831	-0.0066

It is interesting that the air treatments, which are known to cause oxygen solution in the alloy, result in a lattice contraction. This rather unexpected result may mean that oxygen atoms can occupy lattice sites, and because the oxygen atoms (or ions) are smaller than the metallic atoms, the lattice is contracted near oxygen atoms. This result and its interpretation must be considered tentative at present, until confirmed by additional work.

## GENERAL DISCUSSION

There can be no real doubt that the grain-boundary hardening, and the comparatively shallow bulk hardening, are caused by the presence of oxygen. The oxygen diffuses rapidly down the grain boundaries and more slowly through the bulk perpendicular to the grain boundaries and perpendicular to the gas-alloy interface. In the absence of any direct evidence of an oxide precipitate or some gallium-oxygen clustering in regions of high oxygen concentration, the existence of such complexes can only be inferred. Since oxygen-soaked samples are soft in the as-quenched condition, the hardening cannot be attributed to oxygen in solution. Oxygen is present in the soft as-quenched state, as can readily be shown by reheating to 800°C for a few seconds, after which grain boundaries as far as 600 microns from the surface show hardening. Obviously, the hardening cannot be attributed to oxygen penetration during the short reheating treatment.

The process of hardening can be tentatively pictured as follows:

1. Oxygen diffuses rapidly down grain boundaries, driven by the concentration gradient set up by the oxide film of  $\text{Ga}_2\text{O}_3$  at the surface.
2. Upon quenching from 900°C or above, the oxygen is in solution. Since the amount of oxygen in solution must be very small, no hardening due only to oxygen in solution is observed.
3. Upon aging at temperatures around 850°C or lower, an interaction between gallium and oxygen occurs to form an oxide of gallium or a  $\text{Ga}-\text{O}$  complex. This reaction might be written as  $x\text{O} + \text{Ga} = \text{GaO}_x$ .  $\text{GaO}_x$  could be an oxide, suboxide, or a clustering of oxygen atoms in the vicinity of some of the gallium atoms. It is conceivable that lattice defects play a role in the reaction, and are possibly necessary for the hardening to occur.
4. The free energy of the reaction in (3) is evidently close to zero at 900°C, but the reaction becomes negative at lower temperatures and tends to go to the right.
5. When the reaction product forms, be it clusters, oxide or other complex, it sets up lattice strains nearby because it has a molar volume which is different from gallium in NiGa. In this way, nonuniform stress fields are created, or tetragonal strains are set up, which are known to be an important factor in solid solution hardening.
6. The hardening is in proportion to the amount of oxygen available; hence, the hardening is most pronounced at the gas-metal interface, particularly at grain boundaries, along which diffusion is much faster than through the grains.

The subsequent softening by reheating to about 900°C followed by quenching may occur because at this temperature level, the complex is no longer stable since its free energy of formation is now zero or positive, and the oxygen goes back into solution.

So far, the above mechanism seems reasonable on a qualitative basis, but it does not explain the role played by the stoichiometry of the compound. As pointed out early in the report, the grain-boundary hardening tendency is sharply reduced with decrease in gallium content, below about 50 A/o Ga. While some hardening is still observed somewhat below this "stoichiometric" composition, the magnitude of the effect is much less. This effect may be explained in part by the demonstrated drop in gallium activity which undergoes a sharp change with composition at 50 A/o Ga. One might rationalize this behavior by referring again to the chemical reaction which forms the complex  $\text{O} + \text{Ga} = \text{GaO}_x$ . Assuming some suitable fixed oxygen activity level, an x increase in gallium activity will yield a more negative free energy of formation of  $\text{GaO}_x$ . Or, to put it somewhat differently, a certain minimum gallium activity value must be realized in order to have  $\Delta F_{\text{GaO}_x}$  negative. This may very well be correct, but having no way to estimate the oxygen activity, and not knowing the composition of  $\text{GaO}_x$ , the free energy value cannot be calculated at present.

The tentative mechanism suggested above is possibly similar in nature to the hardening of a silver-aluminum alloy by inward diffusion of oxygen as described by Darken.<sup>(19)</sup> In this system silver alloys containing about 1 per cent Al are caused to dissolve a small amount of oxygen which migrates to the aluminum solute, with the result that each aluminum atom is surrounded by several (up to about 4) oxygen atoms depending upon temperature. No  $\text{Al}_2\text{O}_3$  is formed at temperatures near 300°C because the aluminum cannot diffuse, but the oxygen can move about rather readily. This clustering of oxygen near aluminum atoms causes very pronounced lattice strains and can be measured by lattice parameter measurements. This results in pronounced hardening and strengthening of the silver alloy as compared to the original material without oxygen.

The analogy between this alloy and NiGa is not impressive because of the large difference in active metal concentration in the two cases. However, it is perhaps possible that an analogous mechanism may still operate, although the details must be considerably different. The  $\text{GaO}_x$  complex is much less stable than the  $\text{AlO}_x$  complex in the silver alloy. Even if the mechanism suggested above were actually demonstrated, it still leaves questions relating to the generality of the proposed hardening mechanism and, in particular, a question about the nearly unique behavior of intermetallic compounds. Why do not pure metals, or ordinary solid solutions, show such pronounced grain boundary hardening? Pure metals do show some grain boundary hardening: niobium containing a few tenths per cent oxygen exhibits a few VHN increase in hardness, and pure iron very low in carbon shows a small effect after soaking in air. However, in these systems the magnitude of the effect is very small compared to the increase of about 180 VHN shown in NiGa. Other intermetallics like NiAl and AgMg show large effects.

It is hoped that a study of other intermetallic compounds will give information about the generality of the hardening mechanism, and will provide additional clues regarding the nature of the mechanism.

## CONCLUSIONS

1. It has been shown that the pronounced grain-boundary hardening in NiGa after heat treatment in oxygen or in air is caused in some way by the presence of oxygen.
2. The NiGa bulk material is also hardened, but the effect is limited to a few microns from the gas-metal interface.
3. Oxygen diffuses rapidly down grain boundaries at temperatures between 600° and 1000°C, and thence diffuses less rapidly into the bulk alloy. Approximate oxygen diffusion constants (apparently not strongly temperature-dependent) are  $10^{-12}$  cm<sup>2</sup>/sec for the bulk and  $10^{-5}$  cm<sup>2</sup>/sec for the grain boundary.
4. The hardening reaction is only noticeable in NiGa compositions of about 50 A/o Ga or higher in gallium.
5. Oxygen-treated NiGa is not hard after rapid quenching from 900°C or above, but upon aging at temperatures of 850°C or lower, the hardening reaction occurs.
6. The temperature-dependence of the kinetics of the hardening reaction during aging of oxygen-treated NiGa is complicated, showing three different temperature regions, presumably corresponding to two or more different processes. These processes have not been definitely identified.
7. The activity of gallium is a slow function of composition in the homogeneous NiGa phase up to 50 A/o Ga. As more gallium is added, the activity climbs rapidly to the gallium-rich limit of NiGa.
8. The mechanism of the hardening action has not been definitely established, but a tentative explanation is offered. It is expected that a study of other "pest" systems will throw additional light upon this subject.

## REFERENCES

1. J. H. Westbrook and D. L. Wood, "Embrittlement of Grain Boundaries by Equilibrium Segregation," *Nature*, 192, 1280 (1961).
2. J. H. Westbrook and D. L. Wood, "A Source of Grain Boundary Embrittlement in Intermetallic Compounds," *J. Inst. Metals*, 91, 174 (1962-3).
3. J. H. Westbrook and D. L. Wood, "Pest Degradation of Intermetallic Compounds by Grain Boundary Segregation," GE Research Lab. Rept. No. 63-RL-3324 M.
4. M. Hansen, Constitution of Binary Alloys, 2nd ed., McGraw-Hill Book Co., Inc., New York (1958).
5. H. Bueckle, *Z. Metallk.*, 34, 130 (1942).
6. C. T. Sims, W. D. Klopp, and R. J. Jaffee, *Trans. ASM*, 51, 256 (1958).
7. A. D. LeClaire, *Phil. Mag.*, 42, 468 (1951).
8. John C. Fisher, *J. Appl. Phys.*, 22, 74 (1951).
9. John C. Fisher, private communication.
10. A. J. Bradley and A. Taylor, *Proc. Roy. Soc.*, A159, 56 (1937).
11. James P. Coughlin, "Contributions to the Data of Theoretical Metallurgy," XII; "Heats and Free Energies of Formation of Inorganic Oxides," *Bull. 542, Bur. Mines*.
12. Alvin Glassner, "The Thermochemical Properties of the Oxides, Fluorides and Chlorides to 2500°K," ANL-5750 (Supt. Public Doc.).
13. C. N. Cochran and L. M. Foster, *J. Electrochem. Soc.*, 109, 144 (1962).
14. D. R. Stull and G. C. Sinke, "Thermodynamic Properties of the Elements," ACS, Washington, D. C. (1956).
15. C. J. Frasch and C. D. Thurmond, *J. Phys. Chem.*, 66, 877 (1962).
16. Carl Wagner, Univ. of Goettingen, private communication.
17. S. Kachi, *Sci. Repts. of the Research Inst.*, Tohoku, A7, 351 (1955).
18. W. Trzebiatowski and J. Terpilowski, *Bull. acad. polonaise des sciences*, 3, 391 (1955).
19. L. S. Darken, 1961 Campbell Memorial Lecture, *Trans. ASM*, 54, 600 (1961).

### ADDENDUM

Recent findings since this report was submitted for publication throw doubt on the validity of the diffusion constants cited in Table II. Indeed, there is a serious question whether the hardness contours shown along grain boundaries, transverse to grain boundaries, and even in the bulk alloy are evidence of a concentration gradient of a diffusing species. For the present, it would be best to consider the diffusion evidence as possibly but not probably describing oxygen diffusion. The methods of calculation used are in themselves correct, but as stated in the text, the diffusion calculations are necessarily based upon the assumption that hardness is proportional to concentration of a diffusing species (oxygen in this case). The new evidence makes it appear unlikely that this assumption is correct.

A. U. S.

May 16, 1963

Aeronautical Systems Division, Dir/Materials and Processes, Metals and Ceramics Lab, Wright-Patterson AFB, Ohio  
Rpt No. ASD-TDR-63-309, Pt 1. PEST REACTIONS IN INTERMETALLIC COMPOUNDS: Grain Boundary Hardening in NiGa. Final report. Apr 63, 37 pp. incl. illus., tables, 21 refs.

Unclassified Report

The phenomenon of grain boundary hardening has been explored for the CsCl structure intermetallic compound NiGa. NiGa has a homogeneity range of a few per cent and it was possible to examine the effect of

( over )

1. Intermetallic compounds
2. Grain boundary hardening
3. Oxidation

- I. AFSC Project
- II. Contract No. AF 33 (657)-7980

- III. General Electric Research Laboratory, Schenectady, N.Y.

- IV. A.U. Seybolt

- J.H. Westbrook

- V. Aval fro OTS

- VI. In ASTIA collection

Aeronautical Systems Division, Dir/Materials and Processes, Metals and Ceramics Lab, Wright-Patterson AFB, Ohio  
Rpt No. ASD-TDR-63-309, Pt 1. PEST REACTIONS IN INTERMETALLIC COMPOUNDS: Grain Boundary Hardening in NiGa. Final report. Apr 63, 37 pp. incl. illus., tables, 21 refs.

Unclassified Report

The phenomenon of grain boundary hardening has been explored for the CsCl structure intermetallic compound NiGa. NiGa has a homogeneity range of a few per cent and it was possible to examine the effect of

( over )

1. Intermetallic compounds
2. Grain boundary hardening
3. Oxidation

- I. AFSC Project
- II. Contract No. AF 33 (657)-7980

- III. General Electric Research Laboratory, Schenectady, N.Y.

- IV. A.U. Seybolt

- J.H. Westbrook

- V. Aval fro OTS

- VI. In ASTIA collection

stoichiometry upon the grain boundary hardening due to preferential oxygen diffusion down grain boundaries. While some grain hardening was noticeable just below 50 A/o Ga, the effect was much less pronounced than at 52 A/o Ga.

It was possible to estimate both bulk diffusion and grain boundary diffusion rates for oxygen.

The results suggest that hardening is due to lattice distortions which arise from the formation of a Ga-O complex.

( over )

stochiometry upon the grain boundary hardening due to preferential oxygen diffusion down grain boundaries. While some grain hardening was noticeable just below 50 A/o Ga, the effect was much less pronounced than at 52 A/o Ga.

It was possible to estimate both bulk diffusion and grain boundary diffusion rates for oxygen.

The results suggest that hardening is due to lattice distortions which arise from the formation of a Ga-O complex.